UNIVERSIDADE FEDERAL DE MINAS GERAIS
Escola de Engenharia
Programa de Pós-Graduação em Engenharia Elétrica

Marcus Paulo Silva de Abreu

New Adaptive Cruise Control Strategies

Belo Horizonte

2024

Marcus Paulo Silva de Abreu

New Adaptive Cruise Control Strategies

Thesis presented to the Programa de Pós-Graduação em Engenharia Elétrica at the Universidade Federal de Minas Gerais as a partial requirement for the degree of Doctor in Electrical Engineering.

Orientador: Prof. Dr. Fernando de Oliveira Souza

Belo Horizonte
2024

A162n

Abreu, Marcus Paulo Silva de.
New adaptive cruise control strategies [recurso eletrônico] / Marcus Paulo Silva de Abreu. – 2024.
1 recurso online (83 f. : il., color.) : pdf.

Orientador: Fernando de Oliveira Souza.

Tese (doutorado) – Universidade Federal de Minas Gerais, Escola de Engenharia.

Bibliografia: f. 77-83.

1. Engenharia elétrica – Teses. 2. Direção de automóveis – Teses. 3. Veículos autônomos – Teses. 4. Simuladores (Computadores digitais) – Teses. I. Souza, Fernando de Oliveira. II. Universidade Federal de Minas Gerais. Escola de Engenharia. III. Título.

CDU: 621.3(043)

Ficha catalográfica elaborada pelo Bibliotecário Marcio A. A. Gomes CRB/6 2812
Biblioteca Prof. Mário Werneck, Escola de Engenharia da UFMG

UNIVERSIDADE FEDERAL DE MINAS GERAIS

FOLHA DE APROVAÇÃO

"NEW ADAPTIVE CRUISE CONTROL STRATEGIES"

MARCUS PAULO SILVA DE ABREU

Tese de Doutorado submetida à Banca Examinadora designada pelo Colegiado do Programa de Pós-Graduação em Engenharia Elétrica da Escola de Engenharia da Universidade Federal de Minas Gerais, como requisito para obtenção do grau de Doutor em Engenharia Elétrica. Aprovada em 09 de agosto de 2024. Por:

Prof. Dr. Fernando de Oliveira Souza
DELT (UFMG) - Orientador

Prof. Dr. Armando Alves Neto
DELT (UFMG)

Prof. Dra. Fúlvia Stefany Silva de Oliveira
ICT (UNIFEI)

Prof. Dr. José Mário Araújo
DAS (IFBA)

Prof. Dr. Leonardo Amaral Mozelli
DELT (UFMG)

Prof. Dr. Valter Junior de Souza Leite
DEMDV (CEFET-MG)

Documento assinado eletronicamente por **Fernando de Oliveira Souza**, **Professor do Magistério Superior**, em 09/08/2024, às 12:54, conforme horário oficial de Brasília, com fundamento no art. 5º do Decreto nº 10.543, de 13 de novembro de 2020.

Documento assinado eletronicamente por **Valter Junior de Souza Leite**, **Usuário Externo**,

em 11/08/2024, às 22:18, conforme horário oficial de Brasília, com fundamento no art. 5º do Decreto nº 10.543, de 13 de novembro de 2020.

Documento assinado eletronicamente por **Leonardo Amaral Mozelli**, **Subchefe de departamento**, em 12/08/2024, às 09:47, conforme horário oficial de Brasília, com fundamento no art. 5º do Decreto nº 10.543, de 13 de novembro de 2020.

Documento assinado eletronicamente por **Armando Alves Neto**, **Professor do Magistério Superior**, em 12/08/2024, às 10:26, conforme horário oficial de Brasília, com fundamento no art. 5º do Decreto nº 10.543, de 13 de novembro de 2020.

Documento assinado eletronicamente por **José Mário Araújo**, **Usuário Externo**, em 13/08/2024, às 10:18, conforme horário oficial de Brasília, com fundamento no art. 5º do Decreto nº 10.543, de 13 de novembro de 2020.

Documento assinado eletronicamente por **Fúlvia Stefany Silva de Oliveira**, **Usuária Externa**, em 16/08/2024, às 09:46, conforme horário oficial de Brasília, com fundamento no art. 5º do Decreto nº 10.543, de 13 de novembro de 2020.

A autenticidade deste documento pode ser conferida no site https://sei.ufmg.br/sei/controlador_externo.php?acao=documento_conferir&id_orgao_acesso_externo=0, informando o código verificador **3440635** e o código CRC **4A7FF577**.

Referência: Processo nº 23072.243676/2024-23 SEI nº 3440635

To my parents, my fiancée, and my siblings,
for their support, and encouragement.

ACKNOWLEDGMENTS

I thank my parents, Maria das Graças and Rogério de Abreu, and my siblings, Rafael Pedro and Ana Victória, for the encouragement, support, and care that have been essential to my journey so far and for always being present.

I thank my fiancée, Fabiane Rocha, for her companionship, patience, understanding, and affection, which have been fundamental for me to have the strength to complete this stage of my life.

I thank my advisor, Prof. Fernando de Oliveira Souza, for his teachings, patience, attention, and serenity during the development of this work. I am especially grateful for his understanding during my personal difficulties. The lessons learned from him, in addition to being essential for the success of this journey, will certainly be important for overcoming future challenges.

I would like to thank the members of the examination committee, Prof. Leonardo Amaral Mozelli, Prof. Valter Junior de Souza Leite, and Prof. José Mário Araújo, and, especially for their contributions during the completion of this work, Prof. Armando Alves Neto and Prof. Fúlvia Stefany Silva de Oliveira. I also thank the professors of the Graduate Program in Electrical Engineering at UFMG for their teachings and the excellent academic environment

I would also like to thank INCT InSAC (National Institute of Science and Technology for Autonomous Cooperative Systems), CNPq, and CAPES for their financial support.

"It matters that you don't just give up. While there's life, there is hope."

Stephen Hawking

RESUMO

Empregando sensores embarcados e comunicação sem fio intraveicular, o controle de cruzeiro adaptativo cooperativo (CACC - do inglês, *Cooperative Adaptive Cruise Control*) permite que os veículos em um comboio sigam seus predecessores com precisão, resultando em melhor fluxo de tráfego, segurança e conforto. Por outro lado, o CACC é sensível a falhas na comunicação sem fio. Para abordar esta questão, esta tese propõe um controlador que não requer comunicação sem fio e, portanto, não é afetado por falhas de comunicação. Basicamente, o controlador proposto é um CACC degradado (d-CACC), obtido substituindo a aceleração do veículo anterior no CACC por sua estimativa obtida a partir da aproximação da derivada por diferença finita regressiva de primeira ordem. As condições de análise de estabilidade interna e em cadeia do comboio são derivadas utilizando métodos no domínio da frequência. Em seguida, à luz dessas condições de análise de estabilidade, é apresentado um algoritmo para o projeto do d-CACC proposto. Além disso, este trabalho propõe uma nova lei de controle para sistemas ACC (do inglês, *Cooperative Adaptive Cruise Control*) que proporciona um desempenho competitivo em comparação com o CACC. Com base no d-CACC proposto, a principal novidade é a inserção de um termo representando a diferença de velocidade relativa no vetor de erro de estado e a aceleração do próprio veículo na lei de controle. Os ganhos do controlador são projetados a partir de desigualdades matriciais lineares (LMIs - do inglês, *Linear Matrix Inequalities*), garantindo estabilidade interna e em cadeia. Em ambas as propostas, simulações realizadas no MATLAB® e simulações utilizando o CARLA Simulator, que permite a realização de testes em ambientes urbanos realistas, demonstram a eficácia das metodologias.

Palavras-chave: Comboio de veículos, Controle de Cruzeiro Adaptativo Cooperativo (CACC), Controle de Cruzeiro Adaptativo (ACC), Estabilidade em cadeia, Desigualdade matricial linear (LMI).

ABSTRACT

Employing onboard sensors and vehicle-to-vehicle wireless communication, cooperative adaptive cruise control (CACC) allows vehicles in a platoon to follow their predecessors with precision, resulting in better traffic flow, safety, and comfort. On the other hand, CACC is sensitive to wireless communication failures. To address this issue, this thesis proposes a controller that does not require wireless communication and, therefore, is not affected by communication failures. Basically, the proposed controller is a degraded CACC (d-CACC) obtained by replacing the preceding vehicle's acceleration in the CACC with its estimate derived from first-order backward finite difference approximation. The internal and string stability analysis conditions of the platoon are derived using frequency domain methods. Then, in light of these stability analysis conditions, an algorithm for designing the proposed d-CACC is presented. Furthermore, this work proposes a new control law for ACC systems that provides competitive performance compared to CACC. Based on the proposed d-CACC, the main novelty is the insertion of a term representing the relative speed difference in the state error vector and the vehicle's own acceleration in the control law. The controller gains are designed using linear matrix inequalities (LMI), ensuring internal and string stability. In both proposals, simulations conducted in MATLAB® and simulations using the CARLA Simulator, which allows tests to be carried out in realistic urban environments, demonstrate the effectiveness of the methodologies.

Keywords: Vehicle platooning, Cooperative Adaptive Cruise Control (CACC), Adaptive Cruise Control (ACC), String stability, Linear matrix inequality (LMI)

LIST OF FIGURES

Figure 1 – Heterogeneous vehicular platoon equipped with CACC in a predecessor-follower topology. Each vehicle receives information from the preceding vehicle through wireless communication and from its onboard sensors. 20

Figure 2 – Heterogeneous vehicular platoon in a predecessor-follower topology. Each vehicle takes as input only measurements from its onboard front sensors. 29

Figure 3 – Acceleration of the first follower vehicle governed by the proposed d-CACC and the d-CACC from Ploeg et al. (2015). 40

Figure 4 – Spacing error of the first follower vehicle governed by the proposed d-CACC and the d-CACC from Ploeg et al. (2015). 41

Figure 5 – Controller response curves of the first follower vehicle governed by d-CACC and CACC controllers, with different delay values for d-CACC 41

Figure 6 – Acceleration of the first follower vehicle governed by d-CACC and CACC controllers, with different delay values for d-CACC. 42

Figure 7 – Speed of the first follower vehicle governed by d-CACC and CACC controllers, with different delay values for d-CACC. 42

Figure 8 – Spacing error of the first follower vehicle governed by d-CACC and CACC controllers, with different delay values for d-CACC. 42

Figure 9 – Jerk of the first follower vehicle governed by d-CACC and CACC controllers, with different delay values for d-CACC. 43

Figure 10 – The top figure (a) shows the vehicles acceleration under the CACC subject to communication delay (3.21); the bottom figure (b) shows the vehicles acceleration under the proposed d-CACC (3.4). 44

Figure 11 – The top figure (a) shows the vehicles speed under the CACC subject to communication delay (3.21); the bottom figure (b) shows the vehicles acceleration under the proposed d-CACC (3.4). 45

Figure 12 – The top figure (a) shows the follower vehicles spacing error under the CACC subject to communication delay (3.21); the bottom figure (b) shows the follower vehicles spacing error under the proposed d-CACC (3.4). 46

Figure 13 – Simulation setup in CARLA. 47

Figure 14 – The top figure (a) shows the vehicles acceleration under the CACC (3.1); the bottom figure (b) shows the vehicles acceleration under CACC (3.1) switching with the proposed d-CACC (3.4). 48

Figure 15 – The top figure (a) shows the follower vehicles spacing error under the CACC (3.1); the bottom one (b) shows the follower vehicles spacing error under CACC (3.21) switching with the proposed d-CACC (3.4) at the time instants indicated by the dashed vertical lines. 49
Figure 16 – The figures show the vehicles speed under the proposed d-CACC (3.4), wherein the top figure (a) is considered measurement noise and the bottom figure (b) is considered measurement noise and timing error. . 50
Figure 17 – The figures show the follower vehicles spacing error under the proposed d-CACC (3.4), wherein the top figure (a) is considered measurement noise and the bottom figure (b) is considered measurement noise and timing error. 51
Figure 18 – The top figure (a) shows the vehicles jerk under the d-CACC (3.4); the bottom figure (b) shows the vehicles jerk under CACC (3.1) 52
Figure 19 – The top figure (a) shows the vehicles speed under the d-CACC (3.4); the bottom figure (b) shows the vehicles speed under CACC (3.1) . . . 53
Figure 20 – The top figure (a) shows the vehicles acceleration under the d-CACC (3.4); the bottom figure (b) shows the vehicles acceleration under CACC (3.1) 54
Figure 21 – $\mathcal{D}$-region (in gray). 60
Figure 22 – Open-loop poles marked by small circles and the closed-loop poles marked by x. The shaded area indicates the desired $\mathcal{D}$-region for the system closed-loop pole placement. 62
Figure 23 – Controller response curves governed by ACC (a), ACC (b), and CACC for the first follower vehicle. 63
Figure 24 – Acceleration response curves governed by ACC (a), ACC (b), and CACC for the first follower vehicle. 63
Figure 25 – Speed response curves governed by ACC (a), ACC (b), and CACC for the first follower vehicle. 64
Figure 26 – Spacing error response curves governed by ACC (a), ACC (b), and CACC for the first follower vehicle. 64
Figure 27 – Acceleration response curves of a platoon with seven vehicles using ACC (b) in a heterogeneous platoon. 65
Figure 28 – Speed response curves of a platoon with seven vehicles using ACC (b) in a heterogeneous platoon. 65
Figure 29 – Spacing error of a platoon with seven vehicles using ACC (b) in a heterogeneous platoon. 65
Figure 30 – Simulation setup in CARLA with a homogeneous platoon 66

Figure 31 – The top figure (a) shows the vehicles acceleration under the proposed ACC (4.1); the bottom figure (b) shows the vehicles acceleration under ACC (IOANNOU; CHIEN, 1993) (4.2). 68
Figure 32 – The top figure (a) shows the vehicles speed under the proposed ACC (4.1); the bottom figure (b) shows the vehicles speed under ACC (IOANNOU; CHIEN, 1993) (4.2). 69
Figure 33 – The top figure (a) shows the vehicle spacing error under the proposed ACC (4.1); the bottom figure (b) shows the vehicle spacing error under ACC (IOANNOU; CHIEN, 1993) (4.2). 70
Figure 34 – The top figure (a) shows the vehicles jerk under the proposed ACC (4.1); the bottom figure (b) shows the vehicles jerk under ACC (IOANNOU; CHIEN, 1993) (4.2). 71
Figure 35 – Bode diagram comparing the traditional ACC (IOANNOU; CHIEN, 1993) system and the proposed ACC system with $h = 0.4$ and $\zeta_i = 0.3$. 72

LIST OF TABLES

Table 1 – $\mathcal{L}_2$-norm of the states in a seven-vehicle platoon governed by the controllers CACC (3.21) and d-CACC (3.4) under $u_0(t)$ in (3.22) with $k_p = 0.2$, $k_d = 0.7$, $h = 0.5$, and $\tau = \tau_c = 0.02$. 45
Table 2 – Leader Vehicle Parameters and Specifications 47
Table 3 – Vehicle Parameters and Specifications 66

LIST OF ACRONYMS

ACC	Adaptive Cruise Control
CACC	Cooperative Adaptive Cruise Control
d-CACC	Degraded Cooperative Adaptive Cruise Control
ADAS	Advanced Driver Assistance Systems
V2V	Vehicle-to-Vehicle
V2I	Vehicle-to-Infrastructure
V2X	Vehicle-to-Everything
LMI	Linear Matrix inequality
CTH	Constant Time Headway
DoS	Denial of Service
SISO	Single-Input Single-Output

NOTATION

j	$\sqrt{-1}$
$\mathbb{R}^{m\times n}$	the set of $m \times n$ matrices with real entries
$\mathbb{C}^{m\times n}$	set of $m \times n$ matrices with complex entries
$\det(X)$	determinant of a matrix X
$\sigma(X)$	spectrum of a matrix X
$\sigma(A,\ B)$	set of all generalized eigenvalues of a matrix pair $(A,\ B)$
$\otimes$	Kronecker product
I_n	identity matrix with dimensions $n \times n$
0_n	zero matrix with dimensions $n \times n$
H_∞	H_∞ norm
$\mathcal{D}$-region	region $\mathcal{D}$ for pole placement
e_i	spacing error of the i-th vehicle
a_i	acceleration of the i-th vehicle
v_i	speed of the i-th vehicle
q_i	position of the i-th vehicle
h	time-headway
Δ	difference operator
s	Laplace variable
$\Gamma(s)$	spacing error transfer function
CE	characteristic equation
τ	time delay

CONTENTS

1 Introduction 18
1.1 Objectives 22
1.1.1 Degraded cooperative adaptive cruise control (d-CACC) 22
1.1.2 Adaptive cruise control 23
1.2 Outline of the chapters 23
2 General Fundamentals 25
2.1 Notation 25
2.2 Model 25
2.2.1 Longitudinal vehicle model 25
2.2.2 Leader Vehicle H_∞ norm 27
2.3 Definitions 28
3 A novel degraded cooperative adaptive cruise control 29
3.1 Problem statement 29
3.1.1 Conventional CACC controller 30
3.1.2 Proposed d-CACC 31
3.1.3 Platoon formation error dynamics 32
3.1.4 Control objectives 33
3.2 Main results 34
3.2.1 String stability 34
3.2.2 Internal stability 36
3.2.3 A step-by-step design procedure 38
3.3 Numerical examples 39
3.3.1 Design methodology 39
3.3.2 d-CACC performance 39
3.3.3 Communication time-delay 43
3.3.4 Real-world simulations 44
4 A novel ACC control law 55
4.1 Problem statement 55
4.1.1 Novel control law 55
4.1.2 Control objectives 56
4.2 Main results 57
4.3 Numerical example 61
4.3.1 Design methodology 61
4.3.2 Performance of the proposed ACC 62
4.3.3 String stability in heterogeneous vehicle platoons 63

4.3.4 Real-world simulations 64
4.4 Bode Diagram Analysis of Proposed and Traditional ACC 69
5 Conclusions and Future Directions 73
5.1 Conclusions 73
5.2 Published Works 75
5.3 Future Directions 75
References 77

Chapter 1

Introduction

The limited capacity of highways, combined with population growth, has intensified road traffic, causing several problems such as traffic jams, accidents, increased exhaust emissions, and higher fuel consumption (PLOEG; WOUW; NIJMEIJER, 2014; JIA et al., 2015; TIGANASU et al., 2021). In response to these challenges, technological advancements in the automotive industry over recent years have been leading to enhanced safety, comfort, and reliability in road transportation systems (WANG et al., 2020). Therefore, there is extensive research on Advanced Driver Assistance Systems (ADAS) to deal with such issues, where Adaptive Cruise Control (ACC) and Cooperative ACC (CACC) play important roles. To improve the safety and efficiency of vehicle traffic in longitudinal formations (vehicle platoons), ACC and CACC allow vehicle speed adjustment to maintain a certain distance from the preceding one. This way, fuel consumption is reduced, due to lower aerodynamic drag, and it is possible to increase the number of vehicles in longitudinal formation on the road without reducing safety (AREM; DRIEL; VISSER, 2006; ALAM; GATTAMI; JOHANSSON, 2010; KLANČAR; MATKO; BLAŽIČ, 2011; BERTOZZI; BROGGI; FASCIOLI, 2000). For this purpose, ACC uses only information from onboard sensors and radar. More recently than ACC, CACC generally performs better because it allows the exchange of information between the vehicles such as acceleration, speed, and position, utilizing Vehicle-to-Vehicle (V2V), Vehicle-to-Infrastructure (V2I), and Vehicle-to-Everything (V2X) communication. V2V communication enables the direct exchange of information between vehicles, V2I allows communication between vehicles and road infrastructure (DEY et al., 2016), and V2X encompasses both V2V and V2I, enabling comprehensive connectivity in transportation networks (WANG et al., 2019; NOOR-A-RAHIM et al., 2022). However, CACC is only supported in vehicles equipped with wireless communication devices. This reliance on wireless communication introduces potential vulnerabilities, including network security failures, which can affect the reliability and safety of the system. ACC and CACC strategies have been proposed in the literature based on a myriad of control techniques as model predictive control (JIANG et al., 2017;

SHAKOURI; ORDYS, 2014; MOSHARAFIAN et al., 2021), fuzzy logic (CHEN et al., 2016; MAO et al., 2021), neural networks (CAO et al., 2019; TIAN et al., 2021), and optimization based on genetic algorithm (ALONSO et al., 2010). A comprehensive review of research on ACC and CACC, along with the main control methods, can be found in Yu and Wang (2022) and Wang, Wu and Barth (2018).

The critical point in vehicle platoon controller design is to ensure the internal and string stability of the platoon (ESKANDARIAN; WU; SUN, 2021). The internal stability regards the platoon stability as a single system ensuring that the vehicles reach a specified line formation while moving forward according to the platoon leader speed. A platoon with linearized and time-invariant dynamics continuous-time dynamics is said to be internally stable if and only if all eigenvalues of the closed-loop dynamics lie in the left half of the complex plane (GHASEMI; KAZEMI; AZADI, 2013; ZHENG et al., 2015; LIU et al., 2020). To ensure the internal stability of a vehicle platoon system, Gao et al. (2016), Emirler, Güvenç and Güvenç (2018) designed controllers that place the poles in the $\mathcal{D}$-region (Chilali; Gahinet, 1996). On the other hand, string stability refers to the attenuation of disturbance in the upstream direction (PEPPARD, 1974). In the literature, one can find different notions of string stability. Among them, we can mention Naus et al. (2010), Khatir and Davison (2004), Jin and Orosz (2016), which assume that the platoon system is linear and disturbances act only in the leader vehicle. Whereas in Ploeg et al. (2015), it is assumed that all vehicles in the platoon may be subject to disturbances. In addition, string stability notions have also been discussed from a different perspective based on signal measures leading to H_∞ string stability concerning signal amplitude (SWAROOP; HEDRICK, 1996; ROGGE; AEYELS, 2008; WIT; BROGLIATO, 1999) and $\mathcal{L}_2$ string stability regarding signal energy (NAUS et al., 2010; AL-JHAYYISH; SCHMIDT, 2018; PLOEG et al., 2014; ZHU; ZHAO; HE, 2020; KAYACAN, 2017a). Within this range of purposes, it has been settled in the literature to infer string stability from the limited H_∞ norm of the transfer function between subsequent vehicles. Therefore, the closed-loop string stability is ensured by employing an H_∞ state-feedback controller, easily designed from conditions formulated in terms of linear matrix inequalities (LMI). This method has been used with different control laws in vehicle platoon systems (KAYACAN, 2017b; ZHU; HE; ZHAO, 2019; SCHMIED; COLANERI, 2019; HIDAYATULLAH; JUANG, 2021). Literature reviews on this subject can be found in Stüdli, Seron and Middleton (2017) and Feng et al. (2019).

In Adaptive Cruise Control systems, various communication topologies are employed to enhance the efficiency and safety of vehicle platoons. These topologies define how information flows between vehicles in a platoon, impacting the performance of the control strategies used. Common topologies include predecessor-following, two predecessor-following, bidirectional, leader-following, and a combination of these. Each topology offers distinct advantages and challenges in terms of how quickly vehicles can respond to changes

in speed, string stability, and overall dynamic behavior of the platoon. In the predecessor-following topology, information is propagated through the platoon as each vehicle responds to its immediate predecessor. The Figure 1 illustrates a heterogeneous vehicular platoon equipped with CACC in a predecessor-follower topology. Although, as shown in Figure 1, wireless communication is employed in the predecessor-follower topology when vehicles use CACC, this configuration can still be achieved using direct detection based on sensors, without the need for V2V communication, particularly when wireless communication is unavailable or fails. In the two predecessor-following topology, each vehicle responds to both its immediate predecessor and the vehicle two positions ahead, potentially enhancing stability. The bidirectional topology allows vehicles to receive information from both their predecessor and successor. Conversely, in the leader-following topology, each vehicle receives information directly from the leader, which can improve reaction times. However, in the leader-following topology, maintaining stable communication links can become increasingly difficult as the platoon size increases or obstacles interpose between the vehicles, potentially causing limitations in the effectiveness of this topology. Recent research has demonstrated robustness to various topologies (NETO; MOZELLI, 2024). More comprehensive information about topologies can be found in the works of Darbha, Konduri and Pagilla (2018), Gong, Zhou and Peeta (2019), Gülden and Emirler (2024). In our work, we utilize the predecessor-following topology to leverage its advantages in maintaining stable communication within the platoon on a large scale. Furthermore, since our study focuses on systems that do not utilize wireless communication, this topology is necessary because, in our case, onboard sensors and radars can only access information from nearby vehicles, specifically the predecessors.

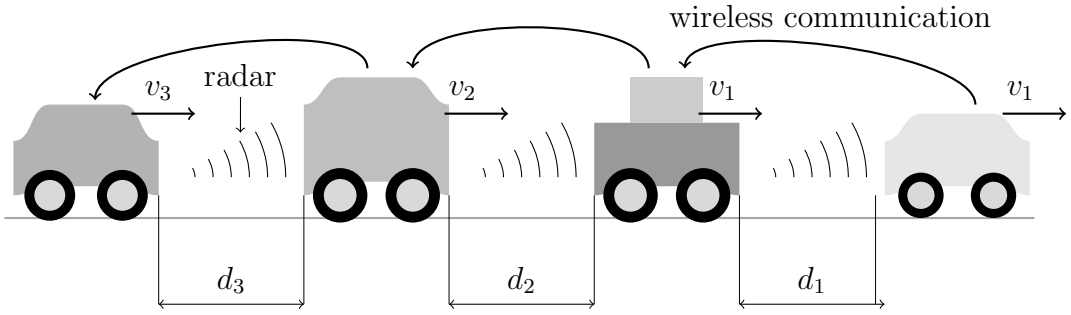

Figure 1 – Heterogeneous vehicular platoon equipped with CACC in a predecessor-follower topology. Each vehicle receives information from the preceding vehicle through wireless communication and from its onboard sensors.

An important aspect to be defined in vehicle platoon control is the spacing policy, which sets the desired distance between vehicles to ensure safety and efficiency. These policies can be categorized into constant and variable spacing policies. The Constant Spacing Policy (CSP) maintains a fixed distance between vehicles, regardless of their speed, and is not suitable for systems that rely solely on onboard sensor measurements

(SWAROOP, 1994). Variable spacing policies adjust the distance based on certain criteria, commonly the vehicle speed, and can be further divided into linear and non-linear policies. Non-linear policies include, among others, the Constant Safety Factor Policy (CSFP) and the Human Driving Behavior Policy (HDBP). The CSFP bases the spacing distance on a safety factor and the safe stopping distance (GARRARD et al., 1978; DARBHA; RAJAGOPAL; TYAGI, 2008), while the HDBP mimics human driving patterns (FANCHER, 2003). Both CSFP and HDBP usually adjust the spacing distance according to the square of the vehicle speed, introducing greater complexity into the closed-loop control dynamics. The Constant Time Headway (CTH) Policy, a linear policy, adjusts the distance between vehicles proportionally to their speed and a constant time interval (time headway). In our work, we utilize the CTH policy due to its balance between safety, simplicity, and traffic efficiency (SWAROOP et al., 1994; SIEBERT; OEHL; PFISTER, 2014). This policy will be detailed further in the thesis. For more information on spacing policies, see Wu et al. (2020).

Regarding the commercially available ADASs, ACC does not ensure string stability in some real situations, as we can see in Gunter et al. (2020). One of the reasons for this is the impossibility of accessing certain information from the preceding vehicle. A hindrance, however, to the popularization of CACC is the need for all platoon vehicles to have wireless communication devices. After all, information such as the acceleration of the preceding vehicle, used in some control laws, can only be obtained by exchanging information between platoon members. A second obstacle is that even though all vehicles have wireless communication devices, wireless data transmission is vulnerable to Denial-of-Service (DoS) attack (PATOUNAS; ZHANG; GJESSING, 2015) and it is subject to faults (TORRENT-MORENO et al., 2009), and/or time-delays that may result in poor performance in the control system (SOUZA et al., 2019; NETO; MOZELLI; SOUZA, 2019). In Ramyar and Homaifar (2019), it is demonstrated that communication failures and packet losses can negatively affect stability. In considering this issue, studies have addressed scenarios of complete disconnection (GODINHO et al., 2023), while others propose methodologies for the control and reorganization of heterogeneous vehicle platoons following vehicle exits and entries (GODINHO et al., 2022). In another approach, several researchers reported in the literature attempts to solve this problem by using acceleration estimates for the preceding vehicle. Hence, vehicle platoon control can be achieved even with the absence of a wireless communication device or when data transmission fails. This is possible because, having the estimative of the preceding vehicle acceleration, further data can be collected via onboard sensors and radar. The fallback controller in the face of wireless communication impairments is known in the literature as degraded CACC (d-CACC). Different techniques have been applied to estimate the preceding vehicle acceleration such as model predictive control based on Gaussian process (MOSHARAFIAN et al., 2021), sliding-mode observer (SAWANT; CHASKAR; GINOYA, 2021), (ROSA et al., 2022), neural networks (TIAN et

al., 2021), Singer's acceleration model, Kalman filter (PLOEG et al., 2015), and adaptive Kalman filter (WU; LIN; ESKANDARIAN, 2019). It can be observed that the methods available in the literature for estimating the acceleration of the preceding vehicle are usually complex or difficult to implement. Furthermore, some papers do not present a systematic method for obtaining the controller gains. In this scenario, this work targets two fronts, whose objectives are detailed in the following subsections.

In response to these challenges, this thesis revisits the control design problem ensuring internal and string stability for heterogeneous ground vehicle platoons by developing a systematic methodology for designing decentralized controller gains. The first proposed control strategy, a degraded Cooperative Adaptive Cruise Control (d-CACC), introduces a constant time delay in the linear feedback control law to estimate the preceding vehicle acceleration via backward difference approximation. This approach avoids numerical differentiation errors and does not require wireless communication. The second proposal, an innovative Adaptive Cruise Control (ACC) system, utilizes only onboard sensor data, incorporating self-vehicle acceleration, relative speed, and spacing error. The proposed control laws results in closed-loop error dynamics independent of the vehicle driveline dynamics, allowing effective application in heterogeneous platoons. The controller gains are designed using Linear Matrix Inequality (LMI) conditions, ensuring H_∞ norm compliance for stability and pole placement in a stable $\mathcal{D}$-region for passenger comfort. Illustrative numerical examples and realistic simulations using MATLAB®, Simulink®, and the CARLA Simulator validate the proposed control laws and design methodologies, demonstrating their practical applicability for real-world implementation. The objectives of each proposal will be addressed separately in the following section.

1.1 Objectives

The general objective of this thesis is to enhance the stability and performance of vehicle platoons by developing robust control strategies relying on vehicle onboard sensors.

To achieve this overarching goal, the thesis focuses on two specific areas of research, which are detailed in the subsections below.

1.1.1 Degraded cooperative adaptive cruise control (d-CACC)

A "degraded mode" is assumed as the operational condition where the system continues to function despite the loss or degradation of certain capabilities. For d-CACC, this means the system must maintain control and stability of the vehicle platoon without relying on inter-vehicle communication. Instead, the system uses onboard sensors and estimation algorithms to infer necessary data, ensuring continuous operation and safety.

In light of this, the main objective is to propose a control law that ensures internal and string stability when the wireless communication device is unavailable or when there is a failure or delay in wireless data transmission. Therefore, the control law must rely only on information available from onboard sensors and radars, operating effectively in degraded mode. As a second objective, the aim is to contribute with a simple systematic methodology for the controller gains design. This approach is detailed in Chapter 3.

1.1.2 Adaptive cruise control

The objective is to propose a control law for ACC systems that offers performance competitive with CACC systems while ensuring internal and string stability. The proposed control law should operate independently of wireless communication between vehicles, relying solely on information from onboard sensors. In this approach, the controller gains are designed based on Linear Matrix Inequality (LMI) conditions in the time domain, ensuring robust performance under various driving conditions.

A key aspect of the proposed control law is to establish a smooth transient response, which is crucial for providing comfort and safety to passengers. This involves minimizing abrupt changes in acceleration and deceleration, thereby enhancing the driving experience. Additionally, the control law should be robust against measurement noise and external disturbances. This approach is detailed in Chapter 4.

By focusing on these objectives, the proposed ACC system aims to bridge the gap between traditional ACC and more advanced CACC systems, providing a viable solution for improving traffic flow and safety without the need for wireless communication infrastructure.

1.2 Outline of the chapters

The sequence of the text is organized as follows:

- Chapter 2 presents the fundamental concepts and notations that serve as the basis for the discussions in the subsequent chapters.
- Chapter 3 presents a systematic methodology for designing the gains of the decentralized CACC controller when inter-vehicle wireless communication fails or is not available (degraded CACC). The proposed methodology is validated by simulations. The results discussed in this chapter generated the published paper Abreu, Oliveira and Souza (2024b).

- In chapter 4, a new ACC control law is proposed with new closed-loop error dynamics, based on the ideas proposed in chapter 3. The proposed control law is also validated by simulations. The results addressed in this chapter generated the published paper Abreu, Oliveira and Souza (2024a).

- Chapter 5 presents the conclusions of the work and future directions.

Chapter 2

General Fundamentals

This chapter outlines the fundamental concepts and notations that serve as the basis for the discussions in the subsequent chapters. It establishes the definitions, models, and terms used throughout this thesis, focusing on general topics that underpin the proposed approaches. Understanding these fundamentals is crucial for following the later sections, which detail the contributions of this work.

2.1 Notation

For a matrix X, denote its determinant by $\det(X)$ and its spectrum by $\sigma(X)$. For a matrix pair $(A,\ B)$, denote the set of all generalized eigenvalues by $\sigma(A,\ B) := \{s \in \mathbb{C} : \det(A - sB) = 0\}$ and the i-th generalized eigenvalue by $\sigma_i(A,\ B)$. The notation $\otimes$ denotes the Kronecker product. Let I_n (0_n) be the identity (zero) matrix with dimensions $n \times n$ and $0_{n\times m}$ the zero matrix with dimensions $n \times m$; throughout the thesis such subscripts may be suppressed, whenever the dimensions are clear from the context.

2.2 Model

This section introduces the longitudinal dynamics model used in this work, which serves as the basis for the proposed control laws.

2.2.1 Longitudinal vehicle model

The following non-linear model is used to represent a vehicle in a longitudinally formed platoon:

$$\begin{aligned} \dot{q}_i(t) &= v_i(t) \\ \dot{v}_i(t) &= a_i(t) \\ \dot{a}_i(t) &= f_i(t) + g_i(t)\mu_i(t), \end{aligned} \tag{2.1}$$

with

$$\begin{aligned} f_i(t) &= -\frac{2K_{di}}{m_i} v_i(t) a_i(t) - \frac{1}{\zeta_i}\left[a_i(t) + \frac{K_{di}}{m_i} v_i^2(t) + \frac{R_{mi}}{m_i}\right] \\ g_i(t) &= \frac{1}{m_i \zeta_i} \end{aligned} \tag{2.2}$$

where

- the subscript i defines the i-th vehicle in the platoon, where $i = 0$ is the index of the leader vehicle;
- $q_i(t)$ represent the rear bumper position of vehicle i;
- $v_i(t)$ represent the speed of vehicle i;
- $a_i(t)$ represent the acceleration of vehicle i;
- $\mu_i(t)$ denotes the engine input of vehicle i;
- m_i represents the mass of vehicle i;
- K_{di} represents the aerodynamic drag coefficient of vehicle i;
- R_{mi} represents mechanical resistance of vehicle i;
- $\zeta_i > 0$ denotes the driveline dynamics of vehicle i.

Given that the parameters in (2.2) are known beforehand, we will use the following state feedback linearization control law, as described by Stankovic, Stanojevic and Siljak (2000),

$$\mu_i(t) = m_i u_i(t) + K_{di} v_i^2(t) + R_{mi} + 2\zeta_i K_{di} v_i(t) a_i(t) \tag{2.3}$$

where $u_i(t)$ is the control input used to set the desired acceleration.

By substituting (2.3) into (2.1), we obtain the following linearized model to describe the longitudinal dynamics of a vehicle platoon (RAJAMANI, 2012):

$$\begin{aligned} \dot{q}_i(t) &= v_i(t) \\ \dot{v}_i(t) &= a_i(t) \\ \dot{a}_i(t) &= -\frac{1}{\zeta_i}a_i(t) + \frac{1}{\zeta_i}u_i(t). \end{aligned} \tag{2.4}$$

The linearized model (2.4) will be utilized in the development of the proposed methods in the following chapters.

2.2.2 Leader Vehicle H_∞ norm

To prove the string and internal stability of the system, we consider the transfer function

$$T_0(s) = \frac{1}{\zeta_0 s + 1} \tag{2.5}$$

which represents the relationship between the desired acceleration and the actual acceleration of the leader vehicle. This transfer function is derived from the dynamic model given in (2.4).

The H_∞ norm of a SISO transfer function $T(s)$ is defined as the maximum gain of the transfer function in the frequency domain, that is,

$$\|T_0(s)\|_{H_\infty} = \sup_{\omega\in\mathbb{R}} |T_0(j\omega)|. \tag{2.6}$$

Replacing s by $j\omega$ in the transfer function (2.5), we obtain:

$$T_0(j\omega) = \frac{1}{\zeta_0 j\omega + 1},$$

thus

$$|T_0(j\omega)| = \left|\frac{1}{\zeta_0 j\omega + 1}\right| = \frac{1}{\sqrt{(\zeta_0\omega)^2 + 1}}.$$

To analyze the behavior of the transfer function $T_0(j\omega)$ across the entire frequency spectrum, we need to examine the limit as ω approaches zero. This approach is true because the magnitude of $T_0(j\omega)$ is a continuous and monotonically decreasing function. Therefore,

$$\lim_{\omega\to 0} |T_0(j\omega)| = 1$$

The H_∞ norm of $T_0(s)$ is 1 for any value of ζ_0:

$$\|T_0(s)\|_{H_\infty} = 1, \quad \forall \zeta_0 \tag{2.7}$$

This result is fundamental to ensuring the system stability before proving string and internal stability. With this verification, we can proceed with the analysis of string and internal stability later in this thesis.

2.3 Definitions

The internal stability of the vehicle platoon system ensures null formation error and same speed in all vehicles in the platoon at the steady-state.

Definition 1 (Internal stability) *A vehicle platoon system is said to be internally stable, i.e., the platoon formation error dynamics are asymptotically stable, if for all* $i = 1, \ldots, m$

$$\lim_{t\to\infty} e_i(t) = 0 \quad \textit{and} \quad \lim_{t\to\infty} \Delta v_i(t) = 0,$$

where $e_i(t)$ is the spacing error between vehicle i and vehicle $i-1$.

The string stability ensures that a disturbance will not be amplified when propagating through the platoon upstream. Therefore, string stability regards a performance criterion essential for scalability purposes. The literature presents different formulations for string stability, see Stüdli, Seron and Middleton (2017), Feng et al. (2019), for instance. In this work, we consider the notion of string stability for predecessor-following topology as stated below.

Definition 2 (String stability) *A vehicle platoon system is said to be string stable if the spacing error of the adjacent vehicles is not amplified along the platoon, whenever the velocity of the leader vehicle changes, namely*

$$||\Gamma_i(j\omega)||_{H_\infty} \leq 1, \ \forall \omega > 0, \ \textit{and} \ i = 1, \ldots, m,$$

where m *is the number of vehicles in the platoon and* $\Gamma_i(s) := e_i(s)/e_{i-1}(s)$.

In this chapter, we have laid the groundwork by defining key mathematical tools and introducing the linearized longitudinal vehicle dynamics model. We have also computed the leader vehicle transfer H_∞ norm. Additionally, we provided definitions for internal and string stability, which will be critical for analysis in subsequent chapters. With these fundamentals in place, we are now in position to explore the design and implementation of control strategies that do not rely on wireless communication, starting with the proposed d-CACC controller in the next chapter and continuing with the ACC controller in the subsequent chapter.

Chapter 3

A novel degraded cooperative adaptive cruise control

This chapter presents a systematic methodology to project the gains of the decentralized controller CACC in the absence of acceleration, denominated degraded CACC (d-CACC). The main novelty of the proposed methodology is the intentional introduction of a constant time delay in the linear feedback control law, which allows an estimative of the preceding vehicle acceleration by first-order backward finite difference approximation. The benefits are twofold: the controller has easy implementation and does not require an inter-vehicle wireless communication device. Unlike other works in the literature, the proposed approach simultaneously guarantees internal and string stability. The proposed design methodology is derived in the frequency domain. Illustrative numerical examples are provided to validate the established control law and its design methodology.

3.1 Problem statement

We consider a platoon with one leader and m heterogeneous following vehicles arranged in a predecessor-follower topology. As shown in Figure 2, where $m = 6$ following vehicles.

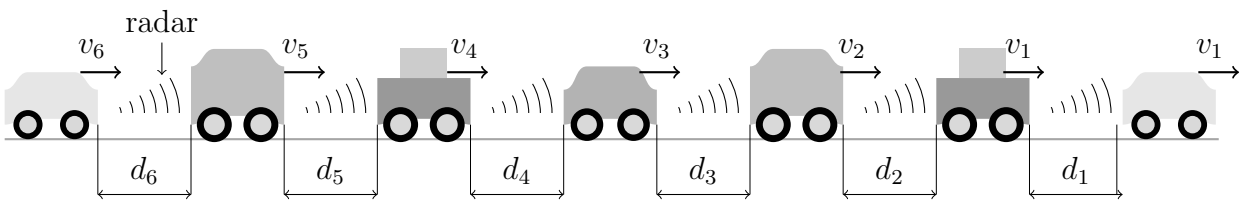

Figure 2 – Heterogeneous vehicular platoon in a predecessor-follower topology. Each vehicle takes as input only measurements from its onboard front sensors.

In this section, we provide a comprehensive overview of the ideas proposed in this chapter. We begin by examining a conventional Cooperative Adaptive Cruise Control (CACC) controller, which serves as the basis for our proposed control law. Next, we introduce our degraded CACC (d-CACC) control law, which addresses potential communication issues of traditional CACC by eliminating the need for predecessor vehicle acceleration data through its approximation. Finally, after a detailed deduction of the closed-loop error dynamics of the vehicles, we define the main control objectives.

3.1.1 Conventional CACC controller

The control problem addressed in this work is to propose and design the control law $u_i(t)$ in (2.4), with $1 \leq i \leq m$, that drive the i-th following vehicle in the platoon to reach a specified line formation, while moving forward according to the platoon leader vehicle speed. In Lefeber, Ploeg and Nijmeijer (2020) it was shown that the following CACC control law can achieve such goal:

$$u_i(t) = \frac{\zeta_i}{h}\left[k_p e_i(t) + k_d \dot{e}_i(t)\right] + \left(1 - \frac{\zeta_i}{h}\right) a_i(t) + \frac{\zeta_i}{h} a_{i-1}(t), \tag{3.1}$$

where $e_i(t)$ is the spacing error, given by

$$e_i(t) = (q_{i-1}(t) - q_i(t) - \ell_i) - d_i(t), \tag{3.2}$$

in which ℓ_i denotes the length of vehicle i and $d_i(t)$ represents the desired distance between vehicle i and its predecessor. Additionally, $d_i(t)$ is formulated as the following constant time-gap spacing policy, which balances simplicity and efficiency, as widely supported in the literature (see, for example, Caudill and Garrard (1977), Seiler, Pant and Hedrick (2004))

$$d_i(t) = r_i + h v_i(t), \tag{3.3}$$

where r_i denotes the standstill distance and $h > 0$ a time gap. We set $\ell_i = r_i = 0$ without loss of generality.

The implicit assumption in the previous control law is the availability of position, velocity, and acceleration measures of the i-th vehicle and its predecessor. In real-world applications, all of these signals can be measured by integrated sensors, e.g., accelerometers and radar, mounted on vehicle i, with the exception of the predecessor vehicle acceleration. The acceleration of the predecessor vehicle can be estimated using onboard sensors; however, this estimation is less reliable and accurate compared to direct communication due to potential sensor noise and inherent delay in the estimation algorithms. Still, the drawback of the previous control law is twofold: all platoon vehicles must be equipped with a wireless module, and, as such, the controller performance is vulnerable to communication

impairments, such as time delay, which degrades the string stability properties (ZHAO et al., 2020).

Therefore, in next section is proposed a design methodology for a simple alternative distributed control law that does not require the availability of the preceding vehicle acceleration. This makes the proposed control law suitable for vehicles without wireless modules and for those operating in environments or situations where communication may fail.

3.1.2 Proposed d-CACC

In this section, we present an alternative control law to cope with the problem of the unavailability of predecessor vehicle acceleration. Our approach is based on the use of first-order backward finite difference to approximate the derivative of signals, as shown next.

Before introducing the proposed control law we point out that the control law (3.1) can be rewritten as

$$\begin{aligned} u_i(t) &= \frac{\zeta_i}{h}\left[k_p e_i(t) + k_d \dot{e}_i(t)\right] + a_i(t) + \frac{\zeta_i}{h}\Delta a_i(t) \\ &= \frac{\zeta_i}{h}\left[k_p e_i(t) + k_d \dot{e}_i(t)\right] + a_i(t) + \frac{\zeta_i}{h}\Delta \dot{v}_i(t), \end{aligned}$$

where $\Delta a_i(t) = a_{i-1}(t) - a_i(t)$ is the relative acceleration and $\Delta \dot{v}_i(t)$ is the time-derivative of the relative speed. Therefore, the last equality reveals that the control law could be implemented using only onboard measurements. However, it is well known that derivatives can hardly be measured directly due to the amplification of high-frequency measurement noise. Further, the numerical differentiation is an ill-posed problem in the Hadamard sense, as such, any small measurement error may cause huge errors in the derivative approximation (HANKE; SCHERZER, 2001; CHENG; JIA; WANG, 2007). Therefore, in order to avoid being subject to unpredictable numerical errors due implementation of the numerical differentiation formula we propose the following alternative d-CACC law

$$u_i(t) = \frac{\zeta_i}{h}\left[k_p e_i(t) + k_d \dot{e}_i(t)\right] + a_i(t) + \frac{\zeta_i}{h\tau}[\Delta v_i(t) - \Delta v_i(t-\tau)], \tag{3.4}$$

where $\tau > 0$ is a small enough scalar. The key idea in proposing this control law is to take into account the effects of the backward derivative approximation

$$\Delta \dot{v}_i(t) \approx \frac{1}{\tau}[\Delta v_i(t) - \Delta v_i(t-\tau)]$$

directly in its design procedure.

As closing point for this section, we emphasize that the main novelty of the proposed d-CACC yields from replacing the preceding vehicle acceleration $a_{i-1}(t)$ in (3.1)

by its backward derivative approximation, as result the proposed d-CACC does not require an in-vehicle wireless communication device, then it is free of wireless communication issues, it does not require extra algorithm for estimate the preceding vehicle acceleration, and it is not subject to unpredictable errors due the formula to estimate the preceding vehicle acceleration.

3.1.3 Platoon formation error dynamics

Let the state error vector $x_i(t) = [e_i(t) \quad \dot{e}_i(t) \quad \Delta v_i(t)]^T$. Then, combining the spacing error definition (3.2), with the vehicle acceleration dynamics (2.4), and the proposed control law (3.4), we can obtain the closed-loop error dynamics of the i-th following vehicle as follows.

Deriving the spacing policy equation (3.2),

$$e_i(t) = q_{i-1}(t) - q_i(t) - hv_i(t) \tag{3.5}$$

$$\dot{e}_i(t) = v_{i-1}(t) - v_i(t) - ha_i(t) \tag{3.6}$$

$$\ddot{e}_i(t) = a_{i-1}(t) - a_i(t) - h\dot{a}_i(t). \tag{3.7}$$

We know that:

$$\Delta v_i(t) = v_{i-1}(t) - v_i(t). \tag{3.8}$$

From (3.6) and (3.8), we then obtain

$$\dot{e}_i(t) = \Delta v_i(t) - ha_i(t) \rightarrow a_i(t) = \frac{1}{h}(\Delta v_i(t) - \dot{e}_i(t)) \tag{3.9}$$

Now, from (3.8) and (3.9),

$$\begin{aligned}\Delta \dot{v}_i(t) &= a_{i-1}(t) - a_i(t) \\ &= a_{i-1}(t) - \frac{1}{h}(\Delta v_i(t) - \dot{e}_i(t)) \\ &= \frac{1}{h}\dot{e}_i(t) - \frac{1}{h}\Delta v_i(t) + a_{i-1}(t).\end{aligned}$$

Substituting $\dot{a}_i(t)$ from (2.4) in (3.7), yields

$$\ddot{e}_i(t) = a_{i-1}(t) - a_i(t) - h[-\frac{1}{\zeta_i}a_i(t) + \frac{1}{\zeta_i}u_i(t)].$$

Now defining $\xi = k_p e_i(t) + k_d \dot{e}_i(t)$ using the proposed control law (3.4), we have

$$\begin{aligned}\ddot{e}_i(t) &= a_{i-1}(t) - a_i(t) + \frac{h}{\zeta_i}a_i(t) - \frac{h}{\zeta_i}\left(\frac{\zeta_i}{h}\xi + a_i(t) + \frac{\zeta_i}{h\tau}[\Delta v_i(t) - \Delta v_i(t-\tau)]\right) \\ &= a_{i-1}(t) - a_i(t) - \left(\xi + \frac{1}{\tau}[\Delta v_i(t) - \Delta v_i(t-\tau)]\right).\end{aligned}$$

Replacing $a_i(t)$ above by (3.9),

$$\begin{aligned}\ddot{e}_i(t) &= a_{i-1}(t) - \frac{1}{h}(\Delta v_i(t) - \dot{e}_i(t)) - \left(\xi + \frac{1}{\tau}[\Delta v_i(t) - \Delta v_i(t-\tau)]\right) \\ &= -\frac{1}{h}(\Delta v_i(t) - \dot{e}_i(t)) - \xi - \frac{1}{\tau}[\Delta v_i(t) - \Delta v_i(t-\tau)] + a_{i-1}(t) \\ &= -\xi - \frac{1}{h}\Delta v_i(t) + \frac{1}{h}\dot{e}_i(t) - \frac{1}{\tau}\Delta v_i(t) + \frac{1}{\tau}\Delta v_i(t-\tau) + a_{i-1}(t) \\ &= -\xi + \frac{1}{h}\dot{e}_i(t) - \left(\frac{1}{h} + \frac{1}{\tau}\right)\Delta v_i(t) + \frac{1}{\tau}\Delta v_i(t-\tau) + a_{i-1}(t).\end{aligned}$$

Finally, we have

$$\dot{x}_i(t) = Ax_i(t) + A_d x_i(t-\tau) + Ba_{i-1}(t), \tag{3.10}$$

with $i = 1, \ldots, m$ and

$$A = \begin{bmatrix} 0 & 1 & 0 \\ -k_p & -k_d + 1/h & -(1/\tau + 1/h) \\ 0 & 1/h & -1/h \end{bmatrix}, \tag{3.11}$$

$$A_d = \begin{bmatrix} 0 & 0 & 0 \\ 0 & 0 & 1/\tau \\ 0 & 0 & 0 \end{bmatrix}, \text{ and } B = \begin{bmatrix} 0 \\ 1 \\ 1 \end{bmatrix}.$$

Note that when we apply the controller (3.4) in the vehicle acceleration dynamics (2.4) the vehicles driveline dynamics ζ_i are canceled. As a result, the closed-loop error dynamics is independent of ζ_i. Therefore, despite of the control law dependence on ζ_i, the following analysis is independent of it.

Accordingly, the formation error dynamics of the overall vehicle platoon system can be modeled as

$$\dot{\mathbf{x}}(t) = \mathbf{A}\mathbf{x}(t) + \mathbf{A_d}\mathbf{x}(t-\tau) + \mathbf{B}\mathbf{u}(t), \tag{3.12}$$

where $\mathbf{A} = I_m \otimes A$, $\mathbf{A_d} = I_m \otimes A_d$, $\mathbf{B} = I_m \otimes B$, $\mathbf{x}(t) = [x_1^T(t), \ldots, x_m^T(t)]^T$, and $\mathbf{u}(t) = [a_0(t), \ldots, a_{m-1}(t)]^T$.

3.1.4 Control objectives

The proposed control law (3.4) aims to ensure both internal and string stability in a cooperative platoon with a predecessor-following topology, as defined in Definitions 1 and 2. To achieve these objectives, the control law focuses on two key aspects. Firstly, the spacing error equation (3.2) is used to demonstrate string stability, preventing the amplification of spacing errors throughout the platoon. Secondly, the formation error dynamics of the overall vehicle platoon system, described by (3.12), is used to prove

internal stability. This design is intended to provide reliable performance and mitigate disturbances, promoting safe and efficient vehicle coordination. By focusing on these stability criteria, the control law addresses key challenges in cooperative driving.

3.2 Main results

In this section we offer the main contributions of the chapter which are based on the d-CACC (3.4).

3.2.1 String stability

The processes for achieving string stability for a desired time gap h are based predominantly on trial and error in the literature to date. In considering this fact, the next theorem presents a sufficient condition that provides a methodical procedure for tuning controller gains such that string stability is ensured for a given h.

Theorem 1 *(String stability condition) Consider a vehicle platoon ruled by the proposed d-CACC in (3.4). Then, the platoon is string stable if*

$$k_p > 0, \tag{3.13}$$
$$k_d \geq \sqrt{2k_p}, \tag{3.14}$$
$$h \geq \tau + \frac{1}{3}k_d\tau^2. \tag{3.15}$$

Proof: Initially choosing the output of the closed-loop system (3.10) as the i-th vehicle acceleration, i.e., $y_i(t) = a_i(t) = Cx_i(t)$, with $C = [0 \ -1 \ 1]/h$. Then, we have the transfer function

$$\begin{aligned} G_i(s) := \frac{a_i(s)}{a_{i-1}(s)} &= C(sI - A - A_d e^{-\tau s})^{-1}B \\ &= \frac{\left(k_d + \frac{(1-e^{-\tau s})}{\tau}\right)s + k_p}{hs^3 + hk_d s^2 + \left(hk_p + k_d + \frac{(1-e^{-\tau s})}{\tau}\right)s + k_p}. \end{aligned}$$

which is independent of i, thus, obviously, $G_i(s) = G_{i-1}(s)$.

Now taking the Laplace transform, assuming zero initial conditions, of the second derivative of the spacing error equation (3.2) we obtain:

$$\begin{aligned} s^2 e_i(s) &= a_{i-1}(s) - a_i(s) - sha_i(s) \\ &= a_i(s)\left(\frac{1}{G_i(s)} - (1 + sh)\right) \end{aligned}$$

and, similarly,

$$\begin{aligned} s^2 e_{i-1}(s) &= a_{i-2}(s) - a_{i-1}(s) - sha_{i-1}(s) \\ &= a_{i-1}(s)\left(\frac{1}{G_{i-1}(s)} - (1+sh)\right), \end{aligned}$$

that yields

$$\Gamma_i(s) := \frac{e_i(s)}{e_{i-1}(s)} = \frac{a_i(s)}{a_{i-1}(s)} \frac{1/G_i(s) + (1-sh)}{1/G_{i-1}(s) + (1-sh)} = G_i(s).$$

Therefore, the string stability condition in Definition 2 can be rewritten as

$$\left|\frac{a_i(j\omega)}{a_{i-1}(j\omega)}\right|^2 \leq 1, \quad \forall \omega \in \mathbb{R},$$

or, equivalently, $|a_{i-1}(j\omega)|^2 - |a_i(j\omega)|^2 \geq 0$, $\forall \omega \in \mathbb{R}$. Now recalling that $e^{-j\tau\omega} = \cos(\tau\omega) - j\sin(\tau\omega)$ and after some simple algebraic manipulations, we have that

$$\begin{aligned} &|a_{i-1}(j\omega)|^2 - |a_i(j\omega)|^2 = \\ &\quad h^2\omega^6 + (h^2k_d^2 - 2hk_d - 2h^2k_p - 2h\tau^{-1})\omega^4 \\ &\quad + (h^2k_p^2 + 2hk_p\tau^{-1})\omega^2 + 2h\tau^{-1}\omega^4\cos(\tau\omega) \\ &\quad + 2hk_d\tau^{-1}\omega^3\sin(\tau\omega) - 2hk_p\tau^{-1}\omega^2\cos(\tau\omega). \end{aligned} \tag{3.16}$$

Further, in view of the second-order Taylor expansion, we have the bounds for the sinusoidal functions.

$$\begin{aligned} 2h\tau^{-1}\omega^4\cos(\tau\omega) &\geq 2h\tau^{-1}\omega^4 - h\tau\omega^6, \\ 2hk_d\tau^{-1}\omega^3\sin(\tau\omega) &\geq 2hk_d\omega^4 - \frac{1}{3}hk_d\tau^2\omega^6, \\ -2hk_p\tau^{-1}\omega^2\cos(\tau\omega) &\geq -2hk_p\tau^{-1}\omega^2. \end{aligned}$$

Then, substituting these bounds in (3.16), we obtain the following sufficient condition for the platoon string stability,

$$\omega^2\left(h\left(h - \tau - \frac{k_d\tau^2}{3}\right)\omega^4 + h^2(k_d^2 - 2k_p)\omega^2 + h^2k_p^2\right) \geq 0$$

for all $\omega \in \mathbb{R}$.

Therefore, the result in the theorem follows by noting that the previous polynomial condition is satisfied for any positive coefficients.

□

3.2.2 Internal stability

Next, we present a lemma providing conditions for internal stability analysis of time-delay systems that is essential to proving the results of this work.

Lemma 1 *(LOUISELL, 2001) Consider the characteristic equation*

$$\mathrm{CE}(s, e^{-s\tau}) = \det(sI - A - A_d e^{-s\tau})$$

of the time-delay system

$$\dot{x}(t) = Ax(t) + A_d x(t-\tau) \tag{3.17}$$

with $A, A_d \in \mathbb{R}^{n\times n}$. *Then the purely imaginary roots of* $\mathrm{CE}(s, e^{-s\tau}) = 0$ *belong to:*

$$j\Omega = \left\{ j\omega_i : j\omega_i \in \sigma\left(\begin{bmatrix} A \otimes I_n & -A_d \otimes I_n \\ I_n \otimes A_d & -I_n \otimes A \end{bmatrix} \right) \right\}.$$

An alternative proof of the previous theorem is found in Souza (2019).

In the following theorem, we present a computable procedure that allows one to determine the largest first time-delay interval for which the closed-loop error dynamics of the i-th vehicle (3.10) preserves its stability.

Theorem 2 (Internal stability condition) *Consider the set* Ω *given in Lemma 1 and the matrices* A *and* A_d *given in* (3.10). *Suppose that* $k_p > 0$ *and* $k_d > 0$.

Define

$$\Phi = \{(\omega_i, \varphi_i) : \ \omega_i \in \Omega \cap \mathbb{R}_+, \ e^{-j\varphi_i} \in \sigma(j\omega_i I - A, A_d) \\ \text{with } \varphi_i \in [0, 2\pi)\}$$

and

$$\tau_{\max} := \begin{cases} \infty, & \text{if } \ \Phi = \emptyset; \\ \min \dfrac{\varphi_i}{\omega_i} & \text{with } (\omega_i, \varphi_i) \in \Phi, \ \text{otherwise.} \end{cases} \tag{3.18}$$

Then the formation error dynamics of the overall vehicle platoon system in (3.12) *is stable for all*

$$\tau \in (0, \tau_{\max}). \tag{3.19}$$

Proof:

The formation error dynamics in (3.12) is asymptotically stable if all roots of the characteristic equation

$$0 = \det\left(sI - \mathbf{A} - \mathbf{A}_d e^{-s\tau}\right),$$

lie in the left half of the complex plane. The matrices $\mathbf{A}$ and $\mathbf{A}_d$ are block diagonal, which means that the dynamics of each vehicle formation error does not directly depend on the states of the other vehicles in the platoon. Each block on the diagonal represents the dynamics of an individual vehicle.

Given that the matrices are block diagonal, the determinant of the entire matrix can be expressed as the product of the determinants of each block. Therefore, we have:

$$\det\left(sI - \mathbf{A} - \mathbf{A}_d e^{-s\tau}\right) = \prod_{i=1}^{m} \det\left(sI - A - A_d e^{-s\tau}\right),$$

revealing that the asymptotic stability of the platoon formation error dynamics (3.12) is dictated by the stability of each vehicle formation error dynamics in (3.10), ruled by the control law (3.4).

Now note that if $k_p > 0$ and $k_d > 0$ then system (3.10) is stable when $\tau \to 0$, because $h > 0$ and

$$\begin{aligned}
&\lim_{\tau\to 0} \mathrm{CE}(s, e^{-s\tau}) = \lim_{\tau\to 0} \det(sI - A - A_d e^{-\tau s}) \\
&= \lim_{\tau\to 0} hs^3 + hk_d s^2 + [hk_p + k_d + \tau^{-1}(1 - e^{-\tau s})]s + k_p \\
&= hs^3 + hk_d s^2 + (hk_p + k_d)s + k_p + \lim_{\tau\to 0} \tau^{-1}(1 - e^{-\tau s})s \\
&= hs^3 + hk_d s^2 + (hk_p + k_d)s + k_p + \lim_{\tau\to 0} \tau^{-1}(1 - e^{-\tau s})s \\
&= hs^3 + hk_d s^2 + (hk_p + k_d)s + k_p + \lim_{\tau\to 0} \left(s^2 - \frac{\tau s^3}{2!} + \frac{\tau^2 s^4}{3!} - \cdots\right) \\
&= hs^3 + hk_d s^2 + (hk_p + k_d)s + k_p + s^2 \\
&= hs^3 + (hk_d + 1)s^2 + (hk_p + k_d)s + k_p
\end{aligned} \tag{3.20}$$

Next, we apply the Routh-Hurwitz criterion to the characteristic polynomial:

$$hs^3 + (hk_d + 1)s^2 + (hk_p + k_d)s + k_p.$$

The Routh array is constructed as follows:

s^3	h	$hk_p + k_d$
s^2	$hk_d + 1$	k_p
s^1	$\dfrac{h^2 k_d k_p + hk_d^2 + k_d}{hk_d + 1}$	0
s^0	k_p	0

For the system to be stable, all the coefficients in the first column must be positive:

- $h > 0$

- $hk_d + 1 > 0$
- $\dfrac{h^2 k_d k_p + h k_d^2 + k_d}{hk_d + 1} > 0$
- $k_p > 0$

We observe that $h > 0$, $k_p > 0$, and $k_d > 0$ satisfy all the conditions. Therefore, the characteristic equation has all its roots in the left half of the complex plane if and only if $h > 0$, $k_p > 0$, and $k_d > 0$. Consequently, $h > 0$, $k_p > 0$, and $k_d > 0$ imply that $\lim_{\tau \to 0} \mathrm{CE}(s, e^{-s\tau}) \neq 0$ for all $s \in \mathbb{C}_+$.

Consider the case $\tau_{\max} \to \infty$ with $\Phi = \emptyset$, and let $\tau > 0$. Lemma 1 implies that $\mathrm{CE}(j\omega, e^{-j\omega\tau}) \neq 0$ for every $\omega > 0$. Because $\mathrm{CE}(0, 1) \neq 0$ for $k_p > 0$, there does not exist $\tau > 0$ such that any root of $\mathrm{CE}(s, e^{-\tau s})$ intersects the imaginary axis. Therefore, because the system (3.10) is stable for $\tau \to 0$, it is stable for any $\tau \in (0,\ \infty)$.

Suppose now that $\tau_{\max} < \infty$. Then $\Phi \neq \emptyset$. By Lemma 1 and under the assumptions that $k_p > 0$ we have that

$$\mathrm{CE}(j\omega_i, e^{-j\omega_i \tau_i}) = \mathrm{CE}(j\omega_i, e^{-j\phi_i}) = 0$$

for each $\omega_i > 0$ and some $\tau_i > 0$ and $\phi_i > 0$. Defining θ_i as the smallest positive ϕ_i we have that $\mathrm{CE}(j\omega_i, e^{-j\omega_i \tau_i}) = 0$ with $\tau_i = \theta_i / \omega_i$, and $\mathrm{CE}(j\omega_i, e^{-j\omega_i \tau_i}) \neq 0$ for any $\tau \in (0,\ \min\{\tau_i\})$. With $\tau_{\max}$ as defined we see now that the system (3.10) is stable for all $\tau \in (0,\ \min\{\tau_i\})$.

Finally, it is clear that $\mathrm{CE}(j\omega_i, e^{-j\omega\tau}) = 0$ for any ω_i is equivalent to $(j\omega_i - A,\ A_d)$ has a generalized eigenvalue of unitary magnitude, $e^{-j\theta_i}$, which is equivalent to $\mathrm{CE}(j\omega_i, e^{-j\theta_i}) = 0$. The proof is now completed.

□

3.2.3 A step-by-step design procedure

In light of Theorems 1 and 2 we propose the following algorithm to design the proposed d-CACC (3.4) ensuring internal and string stability for a cooperative platoon with predecessor-following communication topology.

Algorithm 1 Design procedure for the d-CACC (3.4)

Step 1. Select a small enough delay τ.
Step 2. For a given time gap h, determine k_p and k_d according to the conditions in Theorem 1.
Step 3. Determine if the selected τ belongs to the system stability interval (3.19) according to Theorem 2; otherwise return to Step 1.

3.3 Numerical examples

In this section, numerical examples are presented to illustrate the use of the proposed design methodology, the effectiveness of the proposed d-CACC (3.4), and to show that under communication time-delay, the performance of the proposed controller can be superior to the CACC (3.1). Initially, employing MATLAB® and Simulink® with a maximum step size of 1×10^{-3}, the experiments performed considered a platoon with seven vehicles with longitudinal dynamics in (2.4) where $\zeta_i = 0.1 \ \forall i$, for homogeneous platoon, otherwise $\zeta_i = 0.1(i+1)$, $i = 0, 1, \ldots, 6$; additionally, we set $h = 0.5$ (LEFEBER; PLOEG; NIJMEIJER, 2020).

A seven-vehicle platoon strikes a balance between computational complexity and realism, as real-world platoon formations can vary significantly in size. Then, in the last subsection, 3.3.4, the platoon is simulated by the CARLA (Car Learning to Act) software (DOSOVITSKIY et al., 2017), an open urban driving Simulator that provides a high level of realism with nonlinear vehicle dynamics and environmental interactions.

3.3.1 Design methodology

In order to design the proposed controller (3.4) we follow Algorithm 1. Thus selecting $\tau = 0.3$, it is easy to verify that $k_p = 0.2$ and $k_d = 0.7$, as in Lefeber, Ploeg and Nijmeijer (2020), satisfy the conditions in Theorem 1, that is, the system is string stable with the parameters selected. Finally, we check the internal stability of closed-loop system with the controller parameters $\tau = 0.3$, $k_p = 0.2$ and $k_d = 0.7$. Following Lemma 1 we compute

$$\Omega = \{\pm 3.7980, \ \pm 1.2748\}.$$

Thus, following Theorem 2 it yields

$$\Phi = \{(3.7980, \ 3.5346), \ (1.2748, \ 6.1963)\}$$

and

$$\tau_{\max} = \min \left\{ \frac{3.5346}{3.7980} = 0.93065, \ \frac{6.1963}{1.2748} = 4.8605 \right\}$$

which reveals that the system is internal stable for all $\tau \in (0, \ 0.93065)$. Therefore the controller parameters were selected properly and no interaction of the algorithm is necessary. Namely, the platoon is string and internal stable for $\tau = 0.3$, $k_p = 0.2$ and $k_d = 0.7$.

3.3.2 d-CACC performance

The first proposed method assessment performed was the comparison of the proposed d-CACC controller with a similar one from the literature. Specifically, we

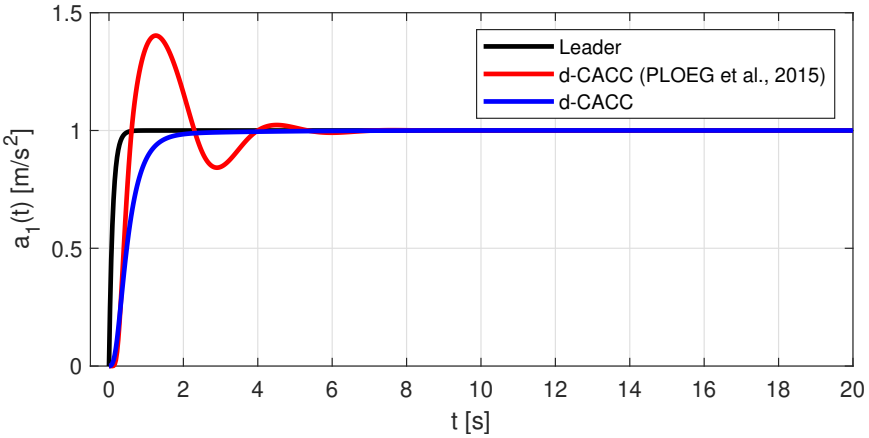

Figure 3 – Acceleration of the first follower vehicle governed by the proposed d-CACC and the d-CACC from Ploeg et al. (2015).

contrasted our controller with the one proposed in Ploeg et al. (2015). This comparison offers a direct view of the performance of our controller in relation to another one that is based on the same basic idea, namely, on the estimation of the acceleration of the preceding vehicle in scenarios where wireless communication is unavailable or fails.

In Ploeg et al. (2015) the control law used for comparison is given in equation (32), Section III-B. The parameters of both controllers used in the simulations are borrowed from Ploeg et al. (2015, Table I), where we get $\zeta_i = 0.1$, $\tau = 0.2$, $k_p = 0.2$, and $k_d = 0.7$. Then, as a result of the previous subsection, we know that the proposed controller (3.4) ensures string and internal stability for the platoon. The additional parameters necessary to implement the Ploeg et al. (2015) control law were defined according to Table I in such paper.

Figure 3 illustrates the acceleration of the first following vehicle governed by these two controllers. Both controllers estimate the acceleration of the lead vehicle without wireless communication; however, notable differences in their dynamic behavior are observed in the simulation results. The d-CACC of Ploeg et al. (2015) yields an oscillatory transient response with high overshoot, which may implicate potential passenger discomfort. Figure 4 shows the spacing error of the d-CACC by Ploeg et al. (2015) and the proposed d-CACC. It is observed that the error with the d-CACC (PLOEG et al., 2015) is greater throughout the simulation and does not converge to zero in steady state. It is important to note that the system developed by Ploeg et al. (2015) is designed exclusively for homogeneous platoons, unlike the system proposed in this work, which is also applicable to heterogeneous systems.

Now we illustrate the influence of time-delay magnitude (τ) on the performance of the proposed d-CACC. To this end, we have selected three different values for τ, namely, $\tau = 0.02$, $\tau = 0.10$, and $\tau = 0.30$. Thus, following the steps of Algorithm 1, we verify that the controller parameters $k_p = 0.2$ and $k_d = 0.7$ satisfy the conditions in Theorem 1 and

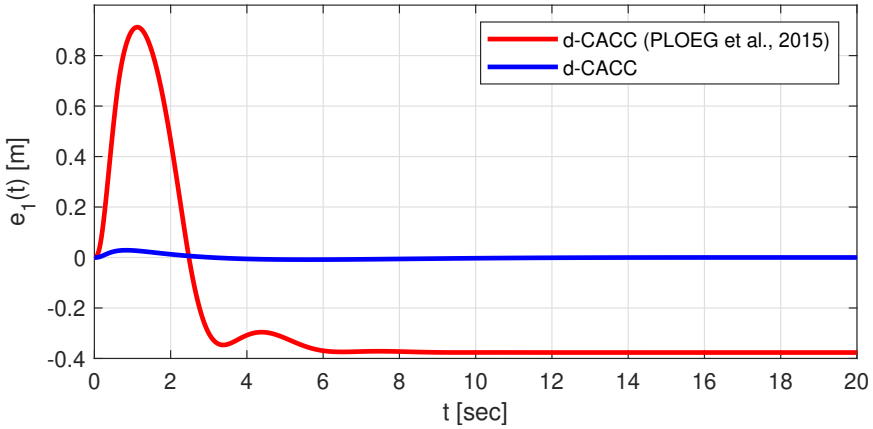

Figure 4 – Spacing error of the first follower vehicle governed by the proposed d-CACC and the d-CACC from Ploeg et al. (2015).

Theorem 2 for all selected values of τ.

Figure 5, Figure 6, and Figure 7 represent the control action $u_1(t)$, the acceleration $a_1(t)$, and the speed $v_1(t)$, respectively, on the first following vehicle due to a step change at times $t = 2s$ and $t = 12s$ in the input of the leader vehicle for the controllers CACC (3.1) and d-CACC (3.4) with various delay values ($\tau = 0.02$, $\tau = 0.10$, and $\tau = 0.30$). Note that, as the value of τ becomes smaller, the response of the d-CACC approaches the CACC. This indicates that the d-CACC with τ properly chosen is an effective solution when the preceding vehicle acceleration is inaccessible.

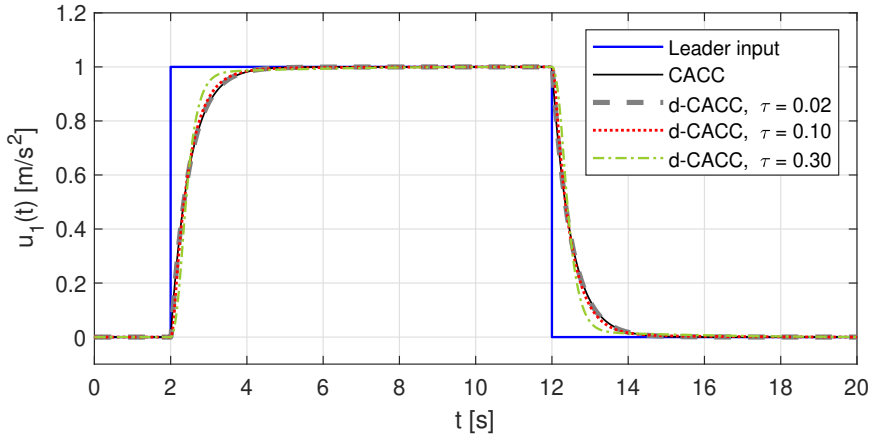

Figure 5 – Controller response curves of the first follower vehicle governed by d-CACC and CACC controllers, with different delay values for d-CACC

Figure 8 and Figure 9 further illustrate the performance of the first follower vehicle relative to the leader under the same conditions. Figure 8 shows the spacing error of the first follower vehicle in relation to the leader. It can be observed that as the delay τ decreases, the spacing error also decreases, becoming closer to the error observed with the traditional CACC, which is nearly zero. This indicates that smaller delay values result in better performance in maintaining the desired spacing between vehicles.

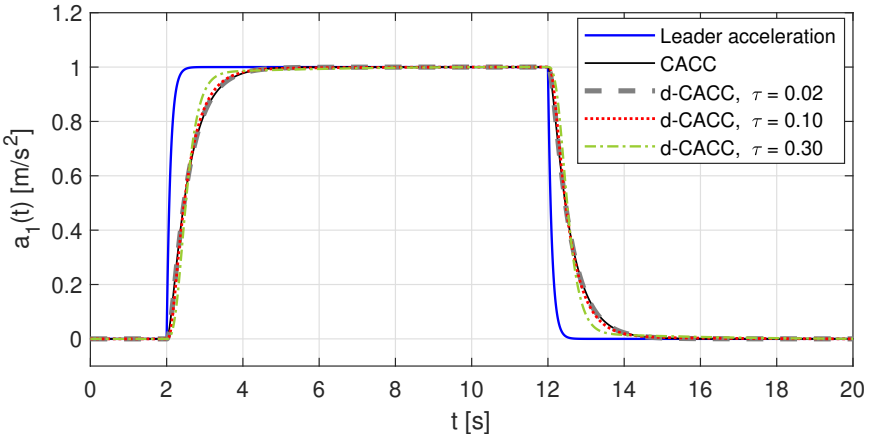

Figure 6 – Acceleration of the first follower vehicle governed by d-CACC and CACC controllers, with different delay values for d-CACC.

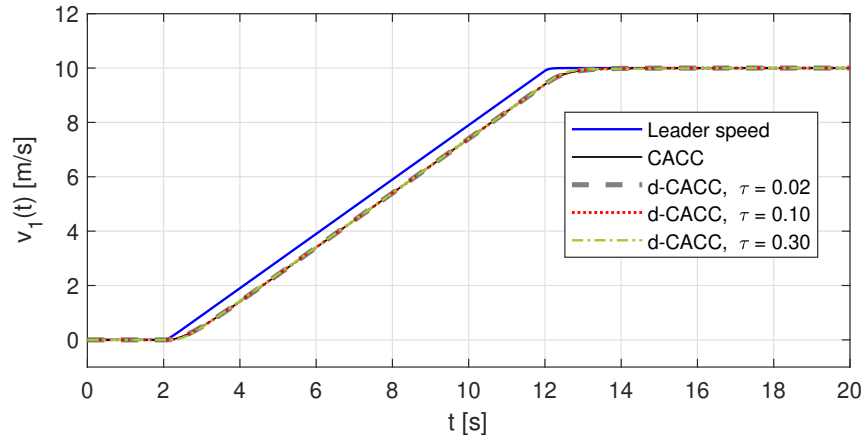

Figure 7 – Speed of the first follower vehicle governed by d-CACC and CACC controllers, with different delay values for d-CACC.

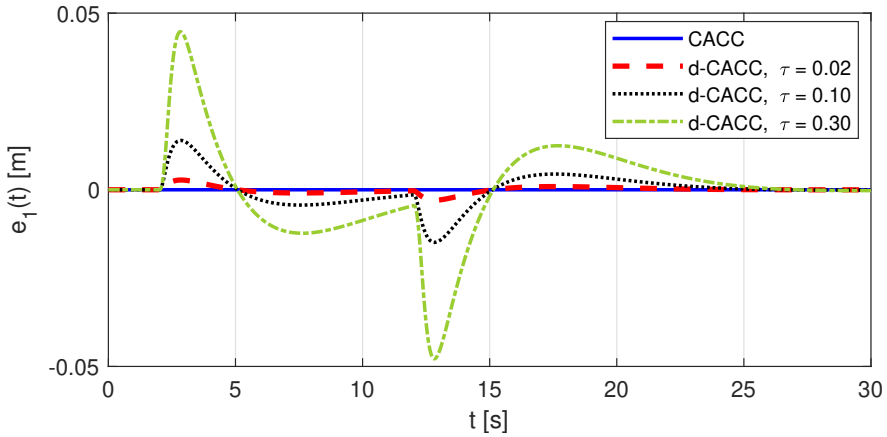

Figure 8 – Spacing error of the first follower vehicle governed by d-CACC and CACC controllers, with different delay values for d-CACC.

Figure 9 displays the jerk of the first follower vehicle in relation to the leader. Jerk is the rate of change of acceleration, and it is a critical measure for assessing passenger

comfort and vehicle wear and tear (HAYATI et al., 2020). Similar to the spacing error, it is evident that the jerk decreases as the delay τ decreases. When $\tau = 0.02$, the jerk is almost identical to that of the traditional CACC, which uses wireless communication between vehicles. This demonstrates that the proposed d-CACC can achieve performance comparable to the traditional CACC in terms of smoothness of acceleration changes, particularly with smaller delay values.

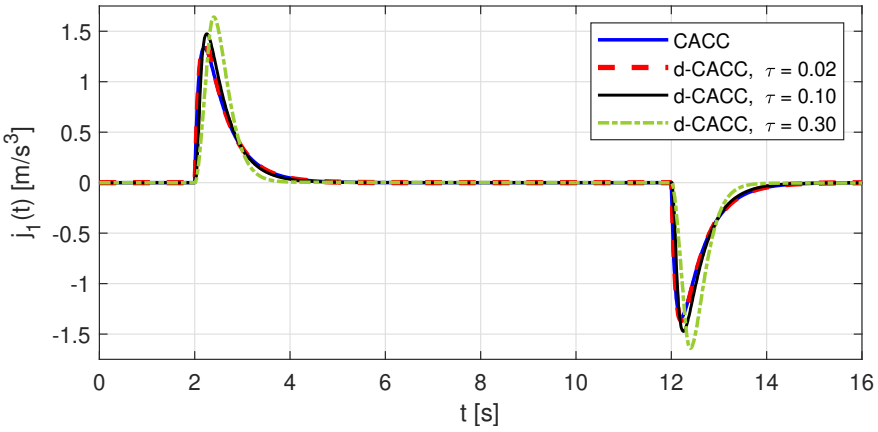

Figure 9 – Jerk of the first follower vehicle governed by d-CACC and CACC controllers, with different delay values for d-CACC.

3.3.3 Communication time-delay

It is noteworthy that the d-CACC (3.4) is not affected by the latency of wireless vehicle-to-vehicle communication which is induced by queueing, contention, transmission, and propagation. However, it is well known that in real applications, the communication delay exists and affects the CACC control (3.1) law as follows:

$$\begin{aligned} u_i(t) &= \frac{\zeta_i}{h}\left[k_p e_i(t) + k_d \dot{e}_i(t)\right] + \left(1 - \frac{\zeta_i}{h}\right) a_i(t) \\ &\quad + \frac{\zeta_i}{h} a_{i-1}(t - \tau_c), \end{aligned} \tag{3.21}$$

where τ_c is the communication delay.

Therefore, we have carried out some simulations with a heterogeneous platoon to compare the performance of the d-CACC with the CACC subject to communication time-delay (3.21), where the leader vehicle is subject to the input

$$u_0(t) = \begin{cases} 1, & 5s \leq t \leq 10s, \\ -1, & 15s \leq t \leq 20s, \\ 0, & \text{otherwise.} \end{cases} \tag{3.22}$$

To compile the results into a convenient form we build the Table 1 listing the $\mathcal{L}_2$-norm of acceleration, speed, and spacing error for the d-CACC with $\tau = 0.02$ and

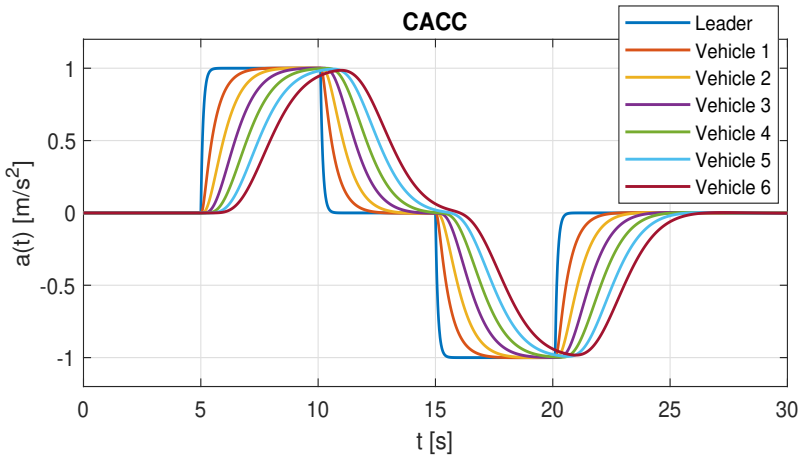

(a)

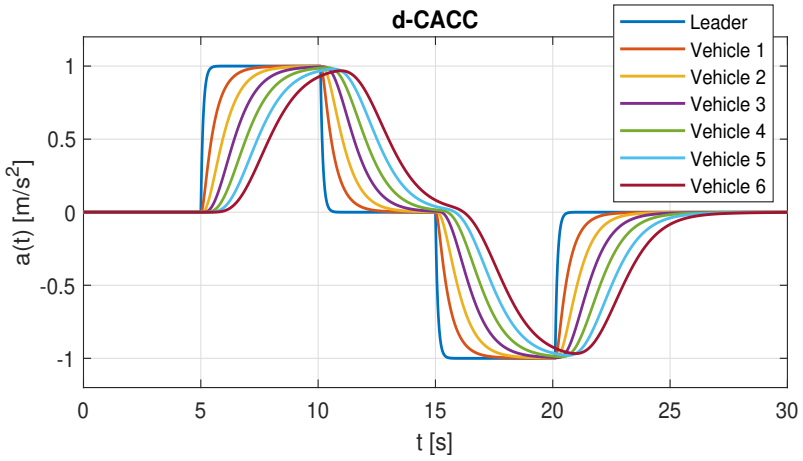

(b)

Figure 10 – The top figure (a) shows the vehicles acceleration under the CACC subject to communication delay (3.21); the bottom figure (b) shows the vehicles acceleration under the proposed d-CACC (3.4).

CACC subject to communication time-delay (3.21) with $\tau_c = 0.02$. According to the $\mathcal{L}_2$-norm the data in Table 1 show that the d-CACC performs slightly better in terms of attenuation of acceleration and speed than the CACC controller subject to communication delay. On the other hand, the improvement in attenuation of the spacing error is significant, which corroborates the effectiveness of the proposed controller. To illustrate the platoon behavior, Figure 10, Figure 11, and Figure 12 show their acceleration, speed, and spacing error, respectively. In addition, it is worth pointing out that in the presence of larger and/or time-varying communication delays the advantages of the proposed controller can be more significant.

3.3.4 Real-world simulations

In this subsection, to verify the efficiency of the proposed d-CACC, we employ the CARLA Simulator (DOSOVITSKIY et al., 2017), wherein the kinematic parameters are

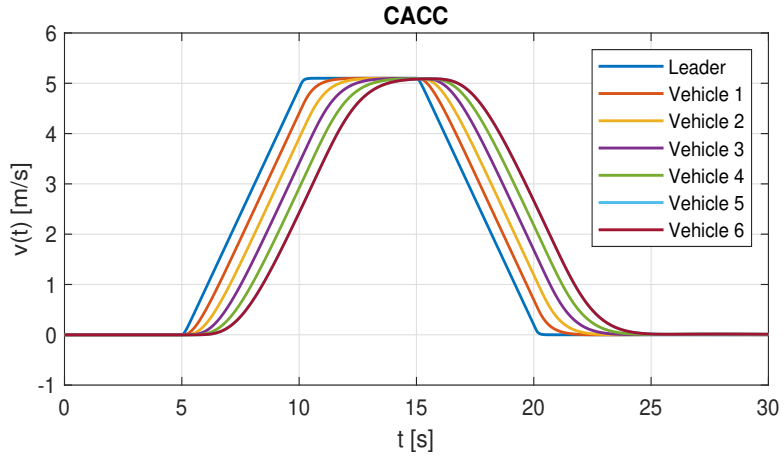

(a)

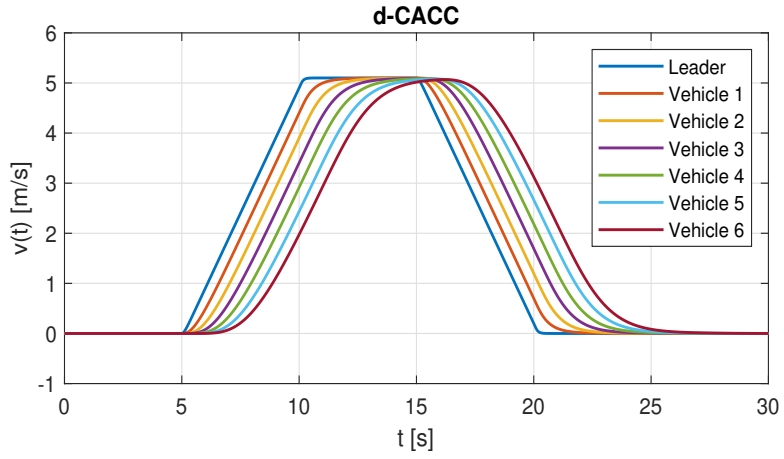

(b)

Figure 11 – The top figure (a) shows the vehicles speed under the CACC subject to communication delay (3.21); the bottom figure (b) shows the vehicles acceleration under the proposed d-CACC (3.4).

Table 1 – $\mathcal{L}_2$-norm of the states in a seven-vehicle platoon governed by the controllers CACC (3.21) and d-CACC (3.4) under $u_0(t)$ in (3.22) with $k_p = 0.2$, $k_d = 0.7$, $h = 0.5$, and $\tau = \tau_c = 0.02$.

	Acceleration		Speed		Spacing error	
Vehicle	CACC	d-CACC	CACC	d-CACC	CACC	d-CACC
0 (Leader)	20.15	20.15	93.47	93.47	-	-
1	19.33	19.27	92.96	92.89	0.489	0.104
2	18.86	18.75	92.47	92.33	0.457	0.095
3	18.50	18.34	92.01	91.80	0.447	0.088
4	18.19	17.99	91.57	91.30	0.439	0.083
5	17.91	17.68	91.16	90.83	0.431	0.079
6	17.65	17.38	90.76	90.38	0.423	0.076

adjusted for realism (DOSOVITSKIY et al., 2017). The use of the CARLA Simulator offers significant advantages for evaluating the controllers. Unlike the simulations in MATLAB®,

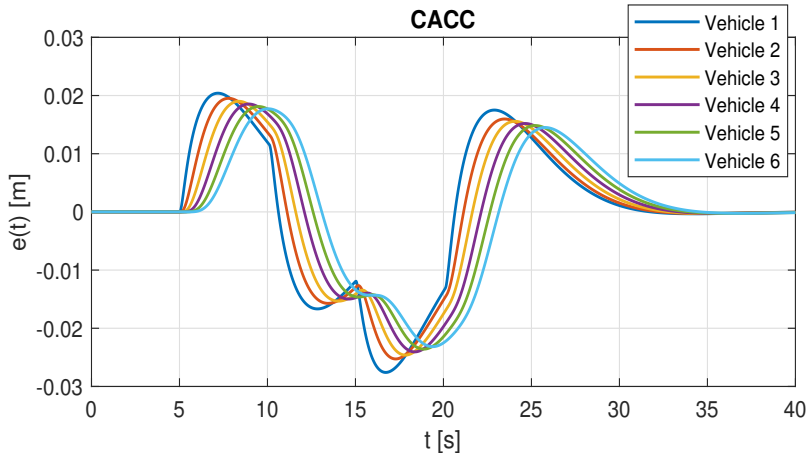

(a)

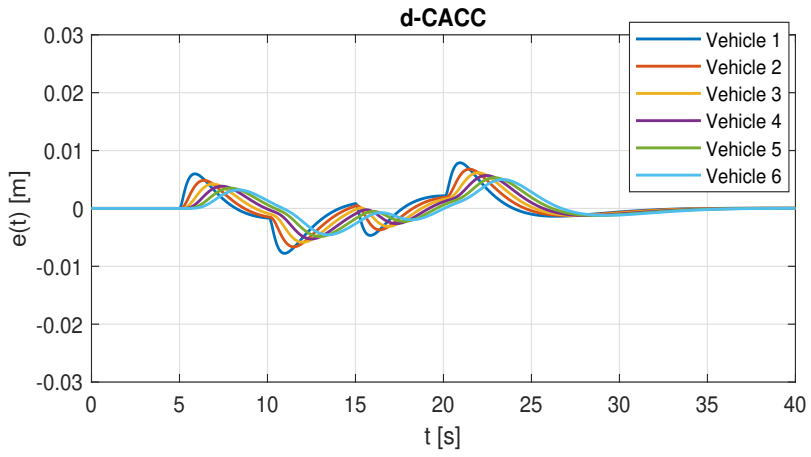

(b)

Figure 12 – The top figure (a) shows the follower vehicles spacing error under the CACC subject to communication delay (3.21); the bottom figure (b) shows the follower vehicles spacing error under the proposed d-CACC (3.4).

which were used linearized models, CARLA implements highly realistic, nonlinear vehicle dynamics models.

The simulations consider a seven-vehicle platoon, as illustrated in Figure 13. The vehicles were simulated on a flat and straight track. We choose $h = 0.5$ and, according to Algorithm 1, we set $k_p = 0.5$, $k_d = 1.05$, and $\tau = 0.1$ in the d-CACC (3.4).

The platoon leader's parameters are detailed in Table 2. It's worth noting that the parameters for the remaining vehicles in the platoon are determined by their respective types and models as defined in the CARLA Simulator.

In addition, all simulations are subject to input delay, namely, the control input is delayed by 0.1. Finally, in order to consider a more challenging case, the leader vehicle is subject to the input

Figure 13 – Simulation setup in CARLA.

Table 2 – Leader Vehicle Parameters and Specifications

Parameter	**Value**
Leader driveline dynamics	0.35
Maximum torque	7500.0 N.m
Mass	1500.0 kg
Drag coefficient	0.4
Wheel radius	0.25 m
Friction constant	0.015
Engine efficiency	80%

$$u_0(t) = \begin{cases} 3.0 & \text{if } 5s \leq t \leq 10s, \\ -1.0 & \text{if } 15s \leq t \leq 20s, \\ 2.0 & \text{if } 25s \leq t \leq 30s, \\ -4.0 & \text{if } 35s \leq t \leq 40s, \\ 0.0 & \text{otherwise.} \end{cases} \tag{3.23}$$

Initially, we illustrate the proposed d-CACC (3.4) being used as a backup controller for the CACC (3.1). To this end, we simulate the platoon governed by the CACC (3.1), where in case of wireless connection interruptions the controller is switched by the proposed d-CACC (3.4). In order to make plain the switching instants in the simulation we consider the switching rule

$$u_i(t) : \begin{cases} \text{CACC}, & \text{if } \sin(t/2) \leq 0, \\ \text{d-CACC}, & \text{otherwise.} \end{cases} \tag{3.24}$$

which leads to the switching instants indicated by the dashed vertical lines in Figure 15(b).

Figure 14 and Figure 15, show, respectively, the acceleration and the spacing error for each vehicle in the platoon, for comparison purposes these figures also show results for the case of the platoon governed only by the CACC (3.1). Thus one can see that the platoon dynamics are similar in both cases, i.e., the proposed d-CACC is capable of mitigating the effects of wireless connection interruptions.

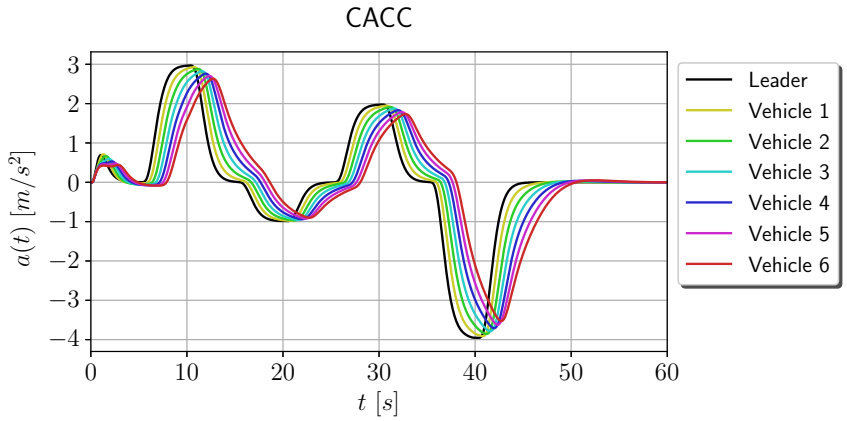

(a)

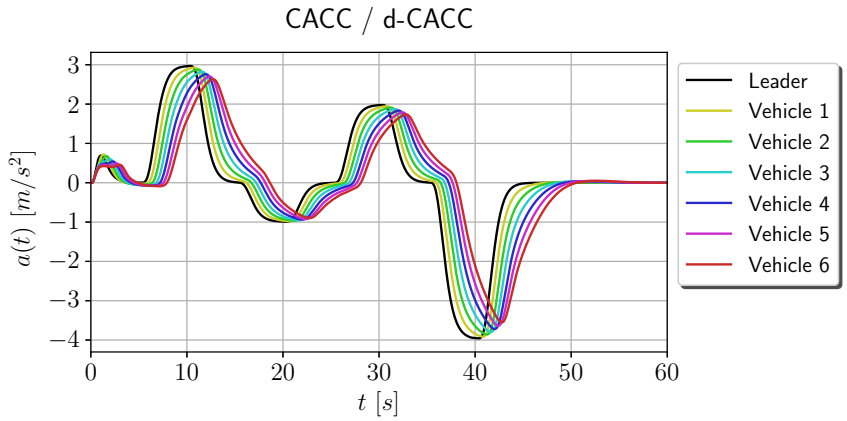

(b)

Figure 14 – The top figure (a) shows the vehicles acceleration under the CACC (3.1); the bottom figure (b) shows the vehicles acceleration under CACC (3.1) switching with the proposed d-CACC (3.4).

Now the aim is to illustrate how the proposed d-CACC (3.4) performs when: (a) there are distance and speed measurement noises, defined as zero-mean white noise process of variance 0.029 and 0.017, respectively, (PLOEG et al., 2015), (b) there exists a timing error to compute the term $\Delta v_i(t-\tau)$, then we replaced it by $\Delta v_i(t-\tau(t))$, where $\tau(t) = \tau + \nu(t)$ with $\nu(t) \in [-0.02,\ 0.02]$.

Figure 16 and Figure 17, show, respectively, the velocity and the spacing error for each vehicle in the platoon, considering both cases. Despite the measurement noise and timing error effects being noticeable in the figures is easy to see that they do not over-change the curve shape. The same occurs when comparing Figure 15 and Figure 17.

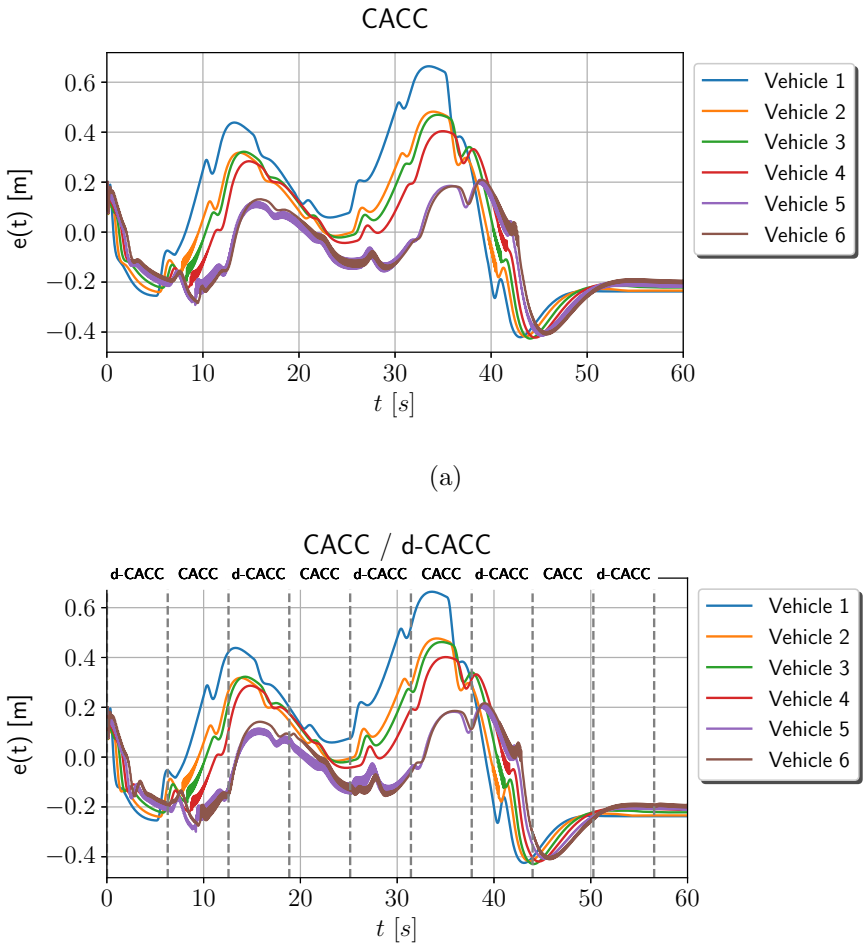

Figure 15 – The top figure (a) shows the follower vehicles spacing error under the CACC (3.1); the bottom one (b) shows the follower vehicles spacing error under CACC (3.21) switching with the proposed d-CACC (3.4) at the time instants indicated by the dashed vertical lines.

Finally, we present simulations that depict a stop-and-start scenario, referencing the following inputs for the lead vehicle:

$$u_0(t) = \begin{cases} 3.0 & \text{if } 5s \leq t \leq 10s, \\ -4.0 & \text{if } 15s \leq t \leq 19s, \\ 4.0 & \text{if } 20s \leq t \leq 25s, \\ -2.0 & \text{if } 30s \leq t \leq 40s, \\ 0.0 & \text{otherwise.} \end{cases} \tag{3.25}$$

Considering that the initial vehicle leader speed is $1m/s$, we can observe that, at the $19.0s$ mark, the vehicles come to a complete stop and remain stationary for an interval of 1 second, resuming acceleration at $20.0s$. These moments of stopping and starting, common in cities, are of paramount importance, as they have a significant

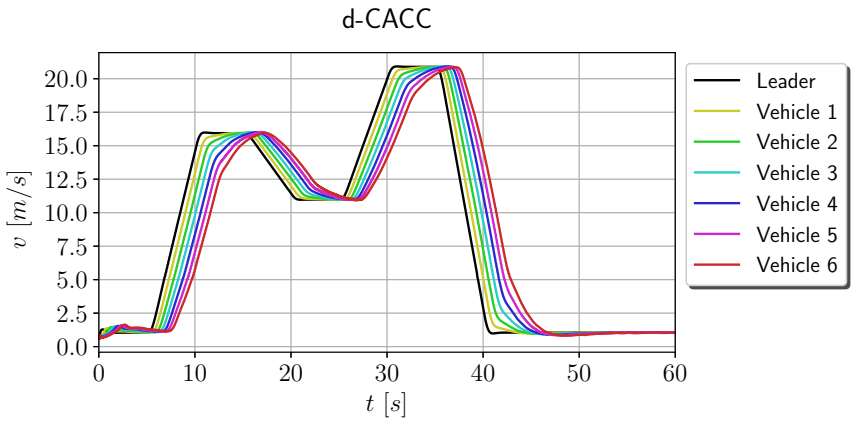

(a)

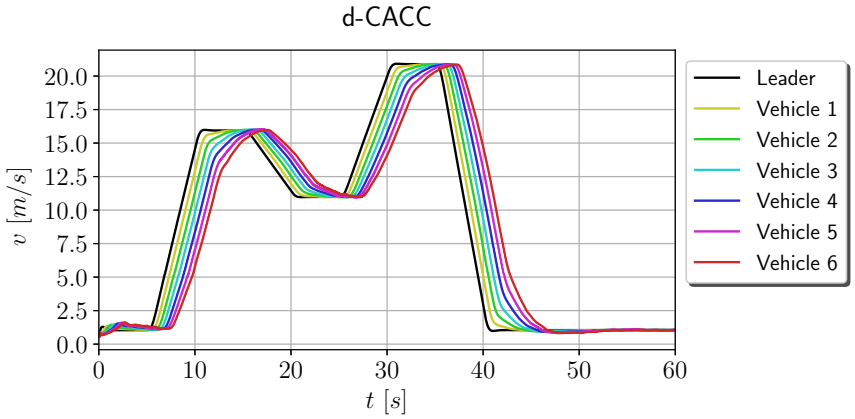

(b)

Figure 16 – The figures show the vehicles speed under the proposed d-CACC (3.4), wherein the top figure (a) is considered measurement noise and the bottom figure (b) is considered measurement noise and timing error.

influence on the jerk, an indicator in determining passenger comfort. Figure 18 illustrates these situations, demonstrating the jerks when applying the d-CACC and the traditional CACC. It's noteworthy that the d-CACC, even without wireless communication, showcases performance similar to the traditional CACC. Additionally, Figs. 19 and 20 depict the speed and acceleration profiles, respectively, for both the traditional CACC and the proposed d-CACC. In Figure 19, we can observe the moment the lead vehicle comes to a complete stop at $t = 19s$, highlighting the system's response to stop-and-start scenarios. Again, these figures show that the d-CACC maintains performance comparable to the traditional CACC system.

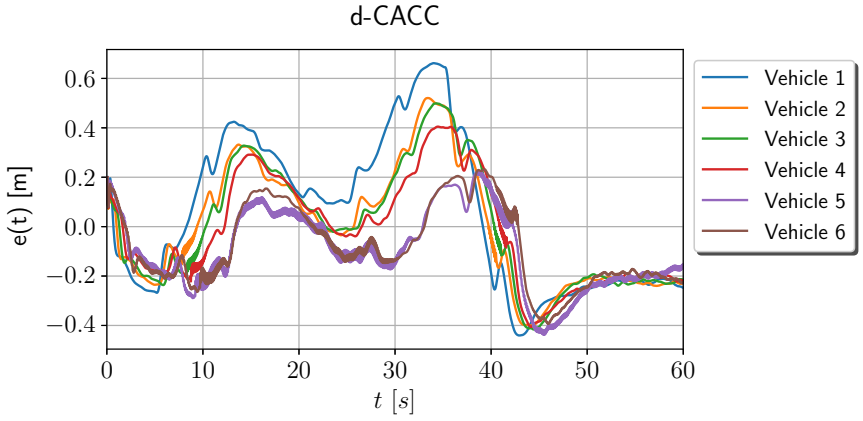

(a)

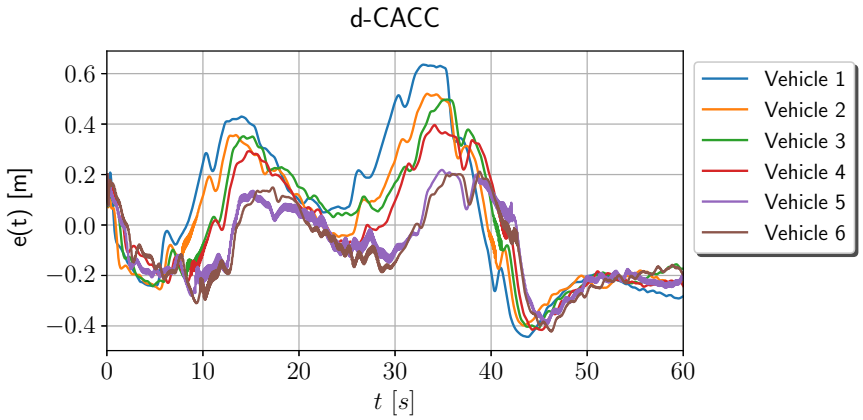

(b)

Figure 17 – The figures show the follower vehicles spacing error under the proposed d-CACC (3.4), wherein the top figure (a) is considered measurement noise and the bottom figure (b) is considered measurement noise and timing error.

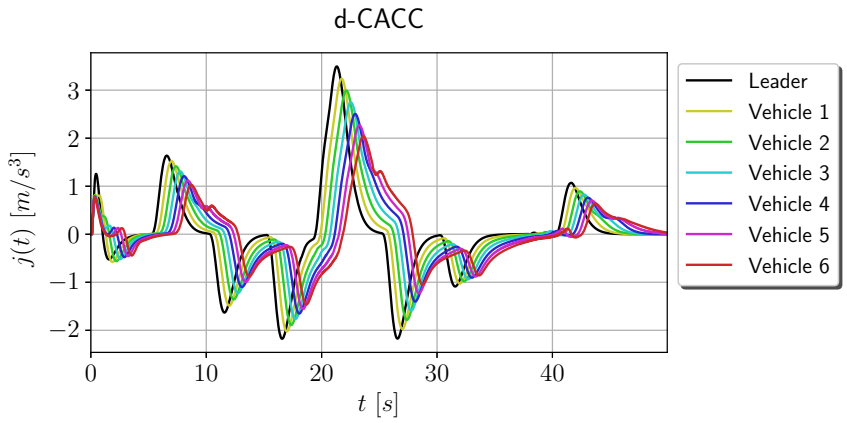

(a)

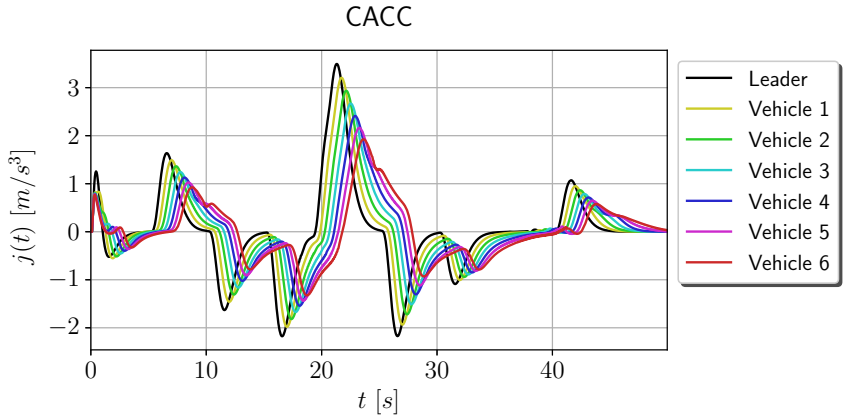

(b)

Figure 18 – The top figure (a) shows the vehicles jerk under the d-CACC (3.4); the bottom figure (b) shows the vehicles jerk under CACC (3.1)

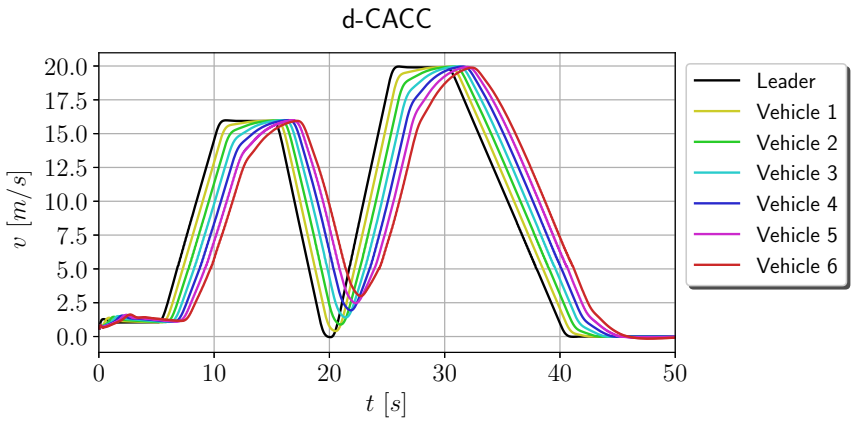

(a)

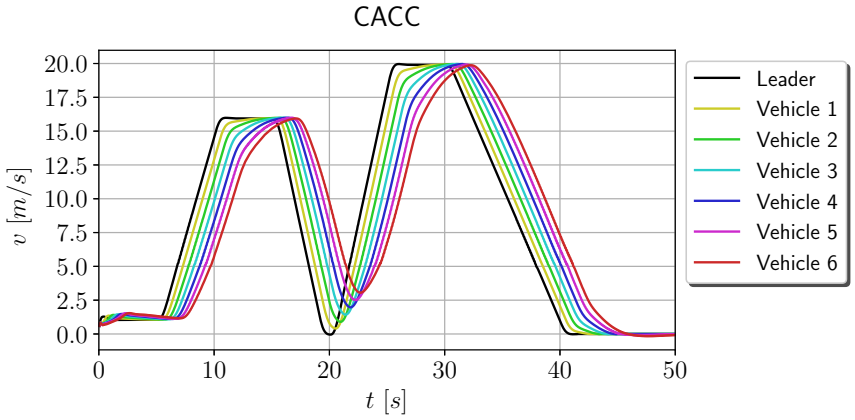

(b)

Figure 19 – The top figure (a) shows the vehicles speed under the d-CACC (3.4); the bottom figure (b) shows the vehicles speed under CACC (3.1)

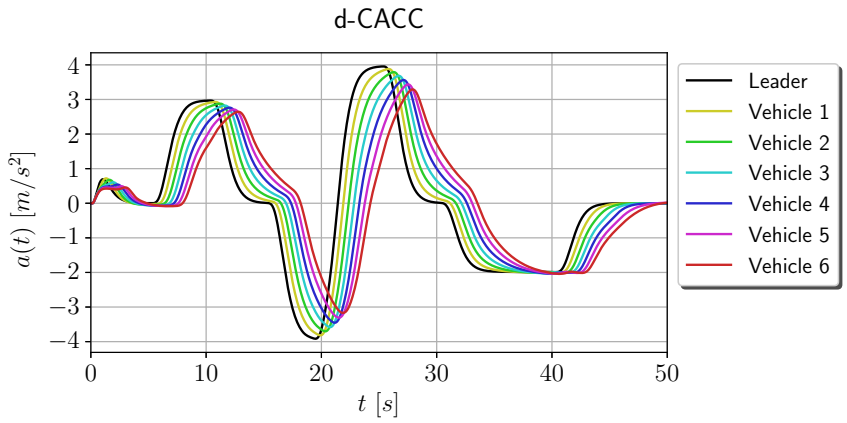

(a)

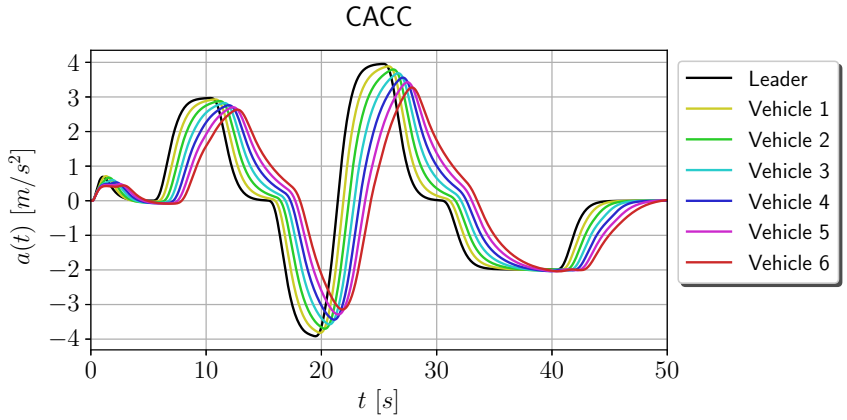

(b)

Figure 20 – The top figure (a) shows the vehicles acceleration under the d-CACC (3.4); the bottom figure (b) shows the vehicles acceleration under CACC (3.1)

Chapter 4

A novel ACC control law

In this chapter, we propose a new control law for cascaded ACC systems to ensure internal and string stability. As with the proposal presented in chapter 3, the controller is easy to implement and does not require wireless communication. The new control law results in closed-loop dynamics that do not depend on the vehicle driveline. Developed from the control law (3.4), the proposed control law also includes the term Δv which represents the difference in speed between two subsequent vehicles and makes it possible not to use the acceleration of the previous vehicle, unlike the well-known CACC control laws. The proposed formulation allows the design of controller gains from LMI conditions. One of the conditions is intended to satisfy the H_∞ norm, which ensures closed-loop string and internal stability. The next three conditions lead to the specification of the vehicle closed-loop error dynamics via pole placement in a stable $\mathcal{D}$-region, which also ensures internal stability and allows the choice of a desired transient response. In this way, it is also possible to focus on passenger comfort, as sudden acceleration and braking can be avoided. Illustrative numerical examples demonstrate the validity of the proposed control law.

4.1 Problem statement

Consider again the model of a platoon with m vehicles given by (2.4).

4.1.1 Novel control law

The following control law is proposed,

$$u_i(t) = a_i(t) + \frac{\zeta_i}{h}\left[k_p e_i(t) + k_d \dot{e}_i(t) + k_v \Delta v_i(t)\right] \tag{4.1}$$

where the scalars k_p, k_d and k_v are the controller gains, $\Delta v_i(t) = v_{i-1}(t) - v_i(t)$ is the speed error, $e_i(t)$ is the spacing error, given by (3.2), and the spacing policy $d_i(t)$ is maintained, as per (3.3). Again, we set $\ell_i = r_i = 0$ without loss of generality.

Considering the widely used ACC control law (IOANNOU; CHIEN, 1993):

$$\mu_i(t) = \frac{1}{h}\left[k_p e_i(t) + \Delta v_i(t)\right] \tag{4.2}$$

the novelties of the proposed control law are the use of the acceleration, the spacing error derivative, and driveline dynamics of vehicle i in the control law. The inclusion of the driveline dynamics results in closed-loop error dynamics independent of vehicle driveline dynamics, that is, for the same controller gains (k_p, k_i, k_v) all vehicles in closed-loop have the same dynamics. In short the proposed ACC control law brings the following benefits:

1. Unrequired wireless communication: no wireless communication module is needed in the controller since the acceleration of the preceding vehicle is not used in the control law. This not only sidesteps challenges related to wireless data reliability, latency, and cybersecurity but also presents potential benefits in terms of reduced system complexity and cost savings.

2. Competitive performance: despite its independence from wireless communication, the proposed ACC exhibits performance metrics that are competitive to traditional CACC systems.

3. Scalability: the proposed control law leads to uniform closed-loop dynamics, independent of each vehicle driveline dynamics. Then, it yields stability conditions even for heterogeneous platoons, which is a significant advantage for scalability.

4. Controller design as LMI conditions: the proposed control law enables the formulation of LMI conditions for determining the controller gains that guarantee both internal and string stability.

5. Transient response shaping: since pole placement constraints can be written as LMI conditions. The flexibility in our methodology allows pole placements, effectively shaping the transient system response. This capability allows for minimizing oscillations and jolts in the dynamics of the vehicles, which has direct implications for enhancing passenger comfort.

4.1.2 Control objectives

The main goals in designing the proposed look-ahead control law (4.1) is to achieve internal and string stability of a vehicle platoon. The internal stability of the

vehicle platoon system ensures null formation error and same speed in all vehicles in the platoon at the steady-state. The string stability ensures that a disturbance will not amplify when propagating through the platoon upstream. Therefore, string stability regards a performance criterion essential for scalability purposes. For the purposes of this chapter, we have defined the string stability as stated in Definition 2.

In addition, because the transient dynamics of a vehicle platoon is directly related with safety, and comfort, the problem under consideration in this chapter is stated as follows.

Problem 1 *Design the look-ahead control law (4.1) for a platoon of vehicles with dynamics in (2.4), such that*

1. *the vehicle platoon system is internally stable according to Definition 1;*
2. *the vehicle platoon system is string stable according to Definition 2;*
3. *the transient response of the vehicle platoon may be somehow specified.*

4.2 Main results

We start this section by writing the closed-loop error dynamics of the i-th following vehicle in the platoon governed by the look-ahead control law (4.1) as a standard linear state-space description. In order to enjoy from the LMI framework to design the gains k_p, k_d, and k_v, of the proposed control law (4.1), in the following we rewrite the present control problem as a standard state-feedback control problem. First, by taking the derivative of the spacing error equation (3.5) and isolating $a_i(t)$, we have that

$$a_i(t) = \frac{1}{h}(\Delta v_i(t) - \dot{e}_i(t)). \tag{4.3}$$

Considering that $\Delta v(t) = v_{i-1}(t) - v_i(t)$, by differentiating, we have

$$\Delta \dot{v}_i(t) = a_{i-1}(t) - a_i(t)$$

Then, using (4.3), it yields

$$\Delta \dot{v}_i(t) = a_{i-1}(t) - \frac{1}{h}\left(\Delta v_i(t) - \dot{e}_i(t)\right). \tag{4.4}$$

Combining the second time derivative of (3.5) and the vehicle dynamics in (2.4), it yields

$$\ddot{e}_i(t) = a_{i-1}(t) - a_i(t) - h[-\frac{1}{\zeta_i}a_i(t) + \frac{1}{\zeta_i}\mu_i(t)]. \tag{4.5}$$

Then, invoking (4.3) again and the proposed control law (4.1), we have that

$$\ddot{e}_i(t) = a_{i-1}(t) - \frac{1}{h}(\Delta v_i(t) - \dot{e}_i(t)) - Kx_i(t) \tag{4.6}$$

where $K = [k_p \;\; k_d \;\; k_v]$ and $x_i(t) = [e_i(t) \;\; \dot{e}_i(t) \;\; \Delta v_i(t)]^T$.

Finally, (4.4) and (4.6) lead to the following controllable system that represents error dynamics in the closed-loop of the i-th following vehicle.

$$\begin{aligned} \dot{x}_i(t) &= Ax_i(t) + B_u u_i(t) + B_a a_{i-1}(t), \\ u_i(t) &= Kx_i(t), \\ a_i(t) &= Cx_i(t), \end{aligned} \tag{4.7}$$

with $i = 1, \ldots, m$,

$$A = \begin{bmatrix} 0 & 1 & 0 \\ 0 & 1/h & -1/h \\ 0 & 1/h & -1/h \end{bmatrix}, B_u = \begin{bmatrix} 0 \\ -1 \\ 0 \end{bmatrix}, B_a = \begin{bmatrix} 0 \\ 1 \\ 1 \end{bmatrix},$$
$$K = \begin{bmatrix} k_p & k_d & k_v \end{bmatrix}, \text{ and } C = \begin{bmatrix} 0 & -1/h & 1/h \end{bmatrix}.$$

Note that by writing the platoon closed-loop error dynamics as the standard linear space-state above, the ACC controller parameters are present only in the static feedback gain vector, K. Consequently, the ACC controller design problem becomes a state feedback controller design problem, on which we can directly apply LMI conditions to solve it. In addition, as a result of the controller (4.1) employment the closed-loop error dynamics is independent of the vehicles driveline dynamics ζ_i. Therefore, once the proposed ACC controller gains are adjusted, the same controller gains can be used in heterogeneous vehicles, the heterogeneity of the vehicles is handled by the driveline dynamics of the vehicles ζ_i in law of control.

Lemma 2 (Internal stability) *A platoon of vehicles with longitudinal dynamics model given in (2.4) governed by look-ahead ACC controller in (4.1) is internally stable according to Definition 1 if and only if the closed-loop error dynamics in (4.7) dropped the index i is asymptotically stable.*

Proof: It follows straight from Definition 1 and the fact that the vehicle closed-loop error dynamics in (4.7) does not change as a function of i. □

In addition, in the same spirit, we establish the following lemma.

Lemma 3 (String stability) *A platoon of vehicles with dynamics given in (2.4) governed by look-ahead ACC controller in (4.1) is string stable according to Definition 2 if and only if*

$$||G(j\omega)||_{H_\infty} \leq 1, \ \forall \omega > 0,$$

where

$$G(s) = \frac{a_i(s)}{a_{i-1}(s)} = \frac{e_i(s)}{e_{i-1}(s)} = C\big(sI - (A + B_u K)\big)^{-1} B_a \tag{4.8}$$

is the transfer function of the closed-loop error dynamics (4.7).

Proof: Keeping in mind that $G(s) = a_i(s)/a_{i-1}(s)$ does not change as a function of i and taking the Laplace transform of the second derivative of the spacing error equation (3.2) we obtain:

$$\begin{aligned} s^2 e_i(s) &= a_{i-1}(s) - a_i(s) - sha_i(s) \\ &= a_i(s)\left(\frac{1}{G(s)} - (1 + sh)\right) \end{aligned}$$

and, similarly,

$$\begin{aligned} s^2 e_{i-1}(s) &= a_{i-2}(s) - a_{i-1}(s) - sha_{i-1}(s) \\ &= a_{i-1}(s)\left(\frac{1}{G(s)} - (1 + sh)\right), \end{aligned}$$

that yields

$$\Gamma(s) = \frac{e_i(s)}{e_{i-1}(s)} = \frac{a_i(s)}{a_{i-1}(s)} \frac{1/G(s) + (1 - sh)}{1/G(s) + (1 - sh)} = G(s).$$

□

The Lemmas 2 and 3 reveal that under the proposed look-ahead control law (4.1) the Definitions 1 and 2 are simplified, since each lemma requires only one test while each definition requires m tests. In addition, because the vehicle closed-loop error dynamics (4.7) is given by a standard linear state-space description, the Lemmas 2 and 3 translate the items i) and ii) of controller design Problem 1 into an H_∞ state-feedback controller design.

Further, because the transient response of a linear time-invariant dynamic system is dictated by the locations of its poles, to deal with the item iii) in Problem 1 we consider a standard $\mathcal{D}$-region for pole assignment resulting by the intersection of: *i*) a half-plane $\mathrm{Re}(s) < -\sigma$, *ii*) a conic sector, and *iii*) a disk with radius ρ, as illustrated in Figure 21.

In the following we state our main result, which is based on the LMI design framework because of its convenience to deal with multiple specifications for the controller design.

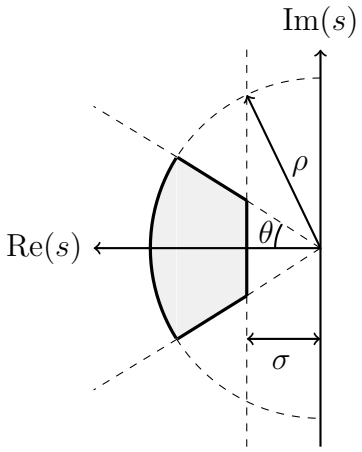

Figure 21 – $\mathcal{D}$-region (in gray).

Theorem 3 *Consider the dynamics in (4.7) and let be given a stable region ($\mathcal{D}$-region), specified by the scalars σ, ρ, and θ, as depicted in Figure 21. The platoon composed by vehicles with dynamics given in (2.4) governed by the look-ahead control law (4.1) is internal and string stable if and only if there exist a symmetric definite positive matrix $P \in \mathbb{R}^{3\times3}$ and a matrix $X \in \mathbb{R}^{1\times3}$ such that*

$$\begin{bmatrix} AP + PA^T + B_uX + X^TB_u^T + B_aB_a^T & PC^T \\ CP & -I \end{bmatrix} \leq 0. \tag{4.9}$$

In addition, the poles of the closed-loop error dynamics in (4.8) belong to the prescribed $\mathcal{D}$-region if the following conditions are also satisfied

$$2\sigma P + AP + PA^T + B_uX + X^TB_u^T < 0, \tag{4.10}$$

$$\begin{bmatrix} -\rho P & AP + B_uX \\ PA^T + X^TB_u^T & -\rho P \end{bmatrix} < 0, \tag{4.11}$$

$$\begin{bmatrix} \sin\theta(\Theta + \Theta^T) & \cos\theta(\Theta - \Theta^T) \\ \cos\theta(\Theta^T - \Theta) & \sin\theta(\Theta + \Theta^T) \end{bmatrix} < 0, \tag{4.12}$$

where $\Theta = AP + B_uX$. In addition, the control law gains are given by $K = [k_p \;\; k_d \;\; k_v] = XP^{-1}$.

Proof: From Lemmas 1 and 2 the problem in the theorem is equivalent to an H_∞ state-feedback controller design with pole assignment specifications. Then the proof of the first part of the theorem statement, which follows directly from the well known Bounded Real Lemma, can be found in Chilali and Gahinet (1996, Sec. III) and Boyd et al. (1994, Sec. 7.5). The proof of the second part of the theorem can be found in Chilali and Gahinet (1996). □

It is important to highlight that the choice to use LMIs for controller design, rather than simpler methods like direct pole placement, offers significant advantages. While some

methods do not allow for simultaneous pole placement and H_∞ optimization, LMIs provide a more flexible and comprehensive approach. The LMI framework enables simultaneous pole placement within a desired region (the $\mathcal{D}$-region) while ensuring H_∞ performance, which is crucial for maintaining robustness and performance in the presence of disturbances. This flexibility makes the LMI approach particularly well-suited for achieving the design objectives of internal and string stability under the proposed control law.

4.3 Numerical example

In this section, numerical examples are presented to illustrate the application of the design methodology and the effectiveness of the proposed ACC controller (4.1). The experiments performed in MATLAB®/Simulink®, with a maximum step size of 1×10^{-3}, considered a heterogeneous platoon with seven vehicles and longitudinal dynamics given in (2.4), where $\zeta_i = 0.1(i+1)$, with $i = 0, 1, \ldots, 6$, and time-gap $h = 0.5$ (LEFEBER; PLOEG; NIJMEIJER, 2020). Additionally, simulations were conducted using the CARLA Simulator to further validate the proposed controller under realistic, nonlinear vehicle dynamics.

4.3.1 Design methodology

In this setup the open-loop error dynamics transfer function, (4.8) setting $K = 0$, has a null and two almost null-poles, as marked in Figure 22 by the circles. It is worth mentioning that if the closed-loop poles cannot be allocated in a specified region, the LMI conditions will not result in a controller. With that in mind, initially, we chose the $\mathcal{D}$-region for pole assignment setting $\rho = 4$, $\theta = \pi/4$, and $\sigma = 0.5$ ($\mathcal{D}$-region (a)), the gray region illustrated in Figure 22 (a). Thus, in order to design the proposed controller (4.1) we apply Theorem 3, which yields

$$P = \begin{bmatrix} 0.2051 & -0.1970 & 0.0105 \\ -0.1970 & 0.5703 & 0.0000 \\ 0.0105 & 0.0000 & 0.5000 \end{bmatrix}$$

and

$$X = \begin{bmatrix} -0.4269 & 2.5808 & 0.0000 \end{bmatrix}$$

and, therefore,

$$K = XP^{-1} = \begin{bmatrix} k_p & k_d & k_v \end{bmatrix} = \begin{bmatrix} 3.3961 & 5.6988 & -0.0716 \end{bmatrix}.$$

As expected the closed-loop system governed by the control law (4.1) with the gains above (ACC (a)) has poles inside the specified $\mathcal{D}$-region (a), as shown in Figure 22 (a).

Likewise, the closed-loop poles can be placed closer to the real axis by decreasing the θ angle of the conic sector of the $\mathcal{D}$-region. In this context, we apply Theorem 3 again with a new set of parameters, $\rho = 7$, $\theta = \pi/6$ and $\sigma = 0.5$, defining the $\mathcal{D}$-region (b) illustrated in Figure 22 (b), which yields

$$P = \begin{bmatrix} 0.0847 & -0.1009 & 0.0213 \\ -0.1009 & 0.5117 & 0.0000 \\ 0.0213 & 0.0000 & 0.5000 \end{bmatrix},$$

$$X = \begin{bmatrix} -0.4991 & 4.1595 & 0.0000 \end{bmatrix},$$

and

$$K = \begin{bmatrix} k_p & k_d & k_v \end{bmatrix} = \begin{bmatrix} 5.0315 & 9.1209 & -0.2146 \end{bmatrix}. \tag{4.13}$$

Now the new control law (ACC (b)) yields closed-loop poles on the real axis, as shown in Figure 22 (b).

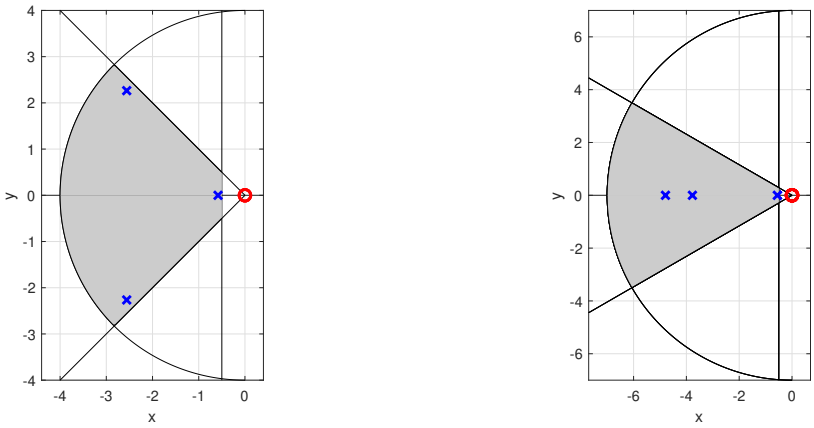

(a) $\rho = 4$, $\theta = \pi/4$ and $\sigma = 0.5$ (b) $\rho = 7$, $\theta = \pi/6$ and $\sigma = 0.5$

Figure 22 – Open-loop poles marked by small circles and the closed-loop poles marked by x. The shaded area indicates the desired $\mathcal{D}$-region for the system closed-loop pole placement.

4.3.2 Performance of the proposed ACC

Here, the transient responses of the system with ACC (a) and (b) have been compared with the transient response of the system governed by a CACC that applies the control law (LEFEBER; PLOEG; NIJMEIJER, 2020)

$$u_i(t) = \frac{\zeta_i}{h}\left[k_p e_i(t) + k_d \dot{e}_i(t)\right] + \left(1 - \frac{\zeta_i}{h}\right) a_i(t) + \frac{\zeta_i}{h} a_{i-1}(t), \tag{4.14}$$

where $a_{i-1}(t)$ is the acceleration of the vehicle ahead received via wireless communication, $k_p = 0.2$ and $k_d = 0.7$. Figure 23, Figure 24, Figure 25 and Figure 26 represent the signal

of the transient response of the control action $u_1(t)$, the acceleration $a_1(t)$, the speed $v_1(t)$, and the spacing error respectively, of the first following vehicle due to a step change at $t = 2s$ and $t = 12s$ in the leader vehicle input for the platoon governed by the ACC (a) and (b) and CACC (4.14). Note that even not using predecessor vehicle acceleration, the proposed ACC controller has a competitive performance compared to CACC.

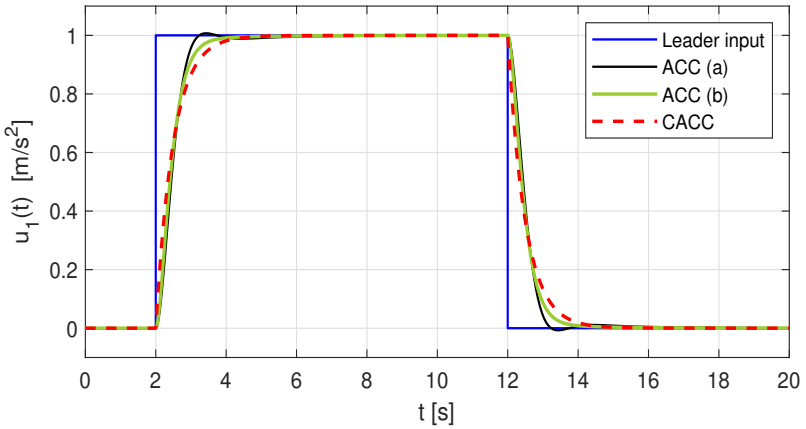

Figure 23 – Controller response curves governed by ACC (a), ACC (b), and CACC for the first follower vehicle.

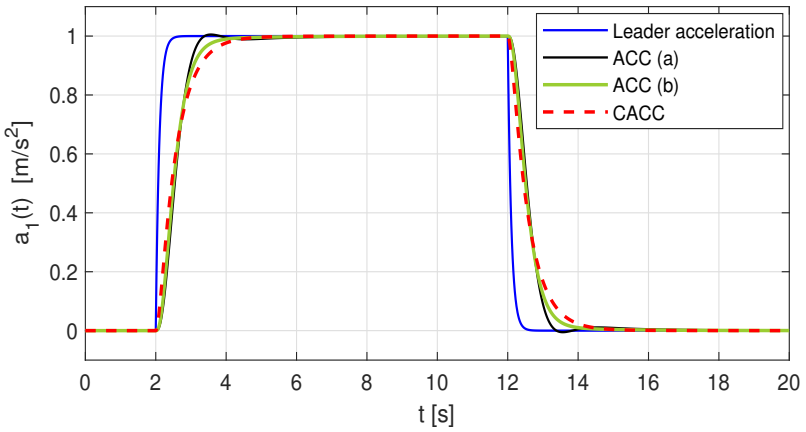

Figure 24 – Acceleration response curves governed by ACC (a), ACC (b), and CACC for the first follower vehicle.

4.3.3 String stability in heterogeneous vehicle platoons

To illustrate string stability maintenance in a heterogeneous platoon, we simulate transient responses of seven vehicles with the leader vehicle subject to the input

$$u_0(t) = \begin{cases} 1, & 5s \leq t \leq 10s, \\ -1, & 15s \leq t \leq 20s, \\ 0, & \text{otherwise.} \end{cases} \tag{4.15}$$

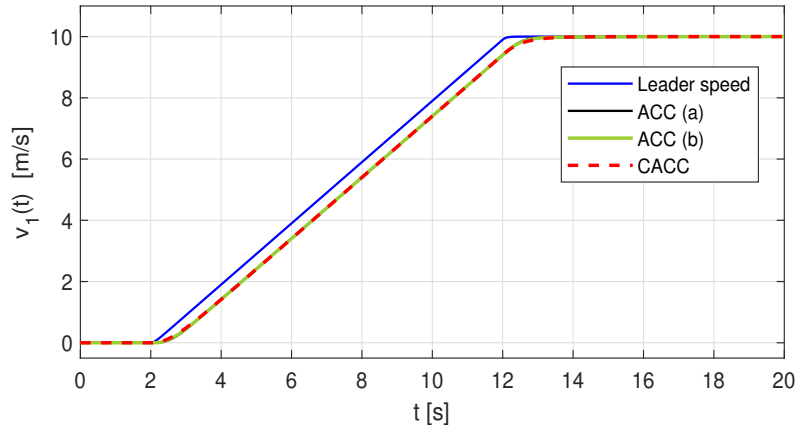

Figure 25 – Speed response curves governed by ACC (a), ACC (b), and CACC for the first follower vehicle.

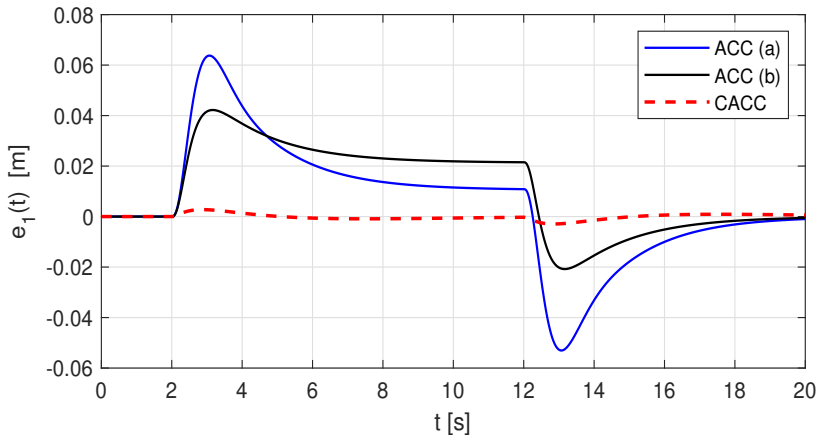

Figure 26 – Spacing error response curves governed by ACC (a), ACC (b), and CACC for the first follower vehicle.

Figure 27, Figure 28, and Figure 29 show the acceleration, speed, and spacing error, respectively, of the seven vehicles In the platoon, using the controller ACC (b) (4.1). As observed, the attenuation of all transient responses along the platoon confirms the string stability, despite the heterogeneous dynamics of the vehicles. In particular, the response behaviors in Figure 29 not only reinforces passenger safety by minimizing variations in the spacing between vehicles, which aids in collision avoidance, but also enhances fuel savings and consequently reduces pollutant emissions, thanks to the efficient aerodynamic formation of the platoon. Such benefits are supported by the study in (DAVILA; ARAMBURU; FREIXAS, 2013).

4.3.4 Real-world simulations

In this subsection, we present simulations of a vehicle platoon using the CARLA Simulator (DOSOVITSKIY et al., 2017). These simulations aim to compare the perfor-

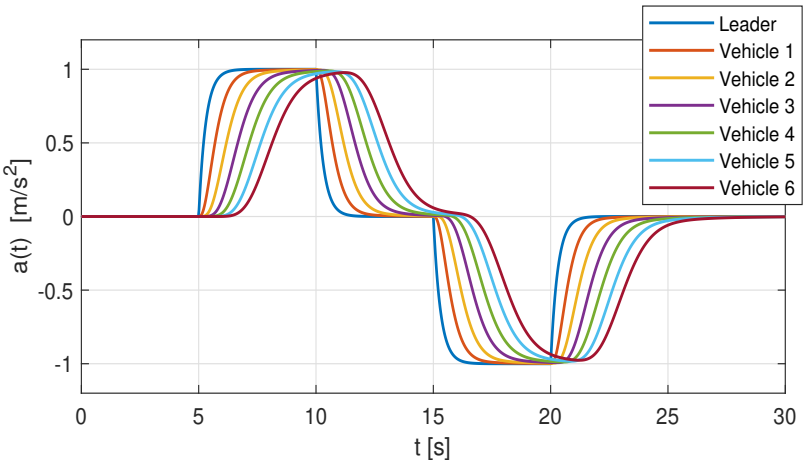

Figure 27 – Acceleration response curves of a platoon with seven vehicles using ACC (b) in a heterogeneous platoon.

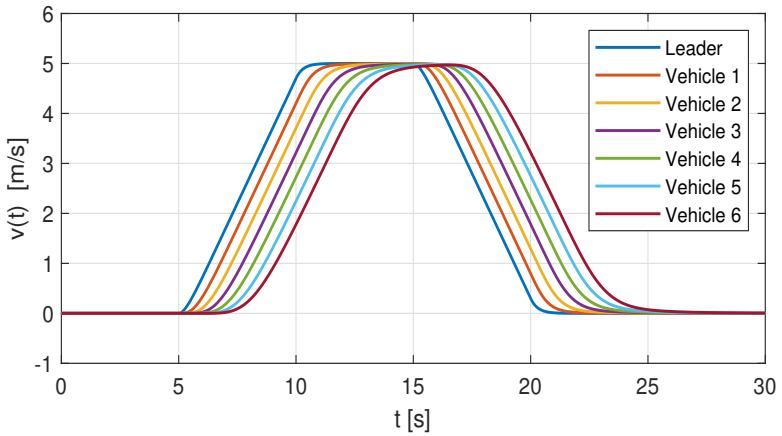

Figure 28 – Speed response curves of a platoon with seven vehicles using ACC (b) in a heterogeneous platoon.

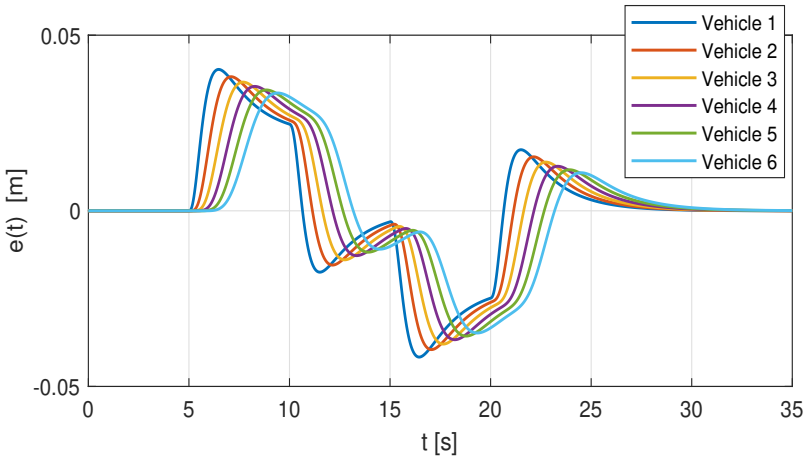

Figure 29 – Spacing error of a platoon with seven vehicles using ACC (b) in a heterogeneous platoon.

mance of a traditional adaptive cruise control system (4.2) by Ioannou and Chien (1993) with the proposed ACC (4.1).

Unlike previous MATLAB® simulations, we opted to use a homogeneous platoon, as illustrated in Figure 30. This choice is because the traditional ACC (4.2), with which we are comparing our proposed ACC, is specifically designed for homogeneous platoons. The parameters of the vehicles in the platoon are detailed in Table 3.

Figure 30 – Simulation setup in CARLA with a homogeneous platoon

Table 3 – Vehicle Parameters and Specifications

Parameter	**Value**
Mass	960.0 kg
Drag coefficient	0.30
Wheel radius	0.34 m
Driveline dynamics	0.15
Friction constant	0.01
Maximum torque	1369.13 N.m
Maximum brake torque	1369.13 N.m

A critical aspect of the simulations is the acceleration pattern used. To represent a more realistic situation, more variations in acceleration were employed compared to the simulation conducted in MATLAB®. We defined a new acceleration pattern that includes both moderate and abrupt accelerations and decelerations, as well as periods of constant speed. This pattern was chosen to represent a variety of situations encountered in real traffic conditions.

Acceleration pattern used:

$$u_0(t) = \begin{cases} 2.0 & \text{if } 2s \leq t \leq 5s, \\ -2.0 & \text{if } 7s \leq t \leq 10s, \\ 5.0 & \text{if } 12s \leq t \leq 15s, \\ -4.0 & \text{if } 17s \leq t \leq 20s, \\ 1.0 & \text{if } 22s \leq t \leq 25s, \\ 0.0 & \text{if } 27s \leq t \leq 30s, \\ -1.0 & \text{if } 32s \leq t \leq 35s, \\ 2.0 & \text{if } 37s \leq t \leq 40s, \\ 0.0 & \text{otherwise.} \end{cases} \tag{4.16}$$

The figures 31, 32, 33, and 34 illustrate the performance of the proposed ACC controller and the traditional ACC controller by Ioannou and Chien (1993) (4.2). The simulations are subject to measurement noise in distance and speed, defined as white noise processes with zero mean and variances of 0.029 and 0.017, respectively (PLOEG et al., 2015). The headway time used in the simulations is $h = 0.5$. The proposed ACC used in the simulations is ACC(b) (4.13), with gains tuned as $k_p = 5.0315$, $k_d = 9.1209$, and $k_v = -0.2146$. For the ACC of Ioannou and Chien (1993), the gain k_p is also set to 5.0315, matching the k_p of the proposed ACC(b).

Figures 31 and 32 show the acceleration and speed patterns of the vehicles, respectively. In subfigure (a) of both figures, the proposed ACC controller is displayed. It can be observed that both acceleration and speed have fewer oscillations, indicating smoother control, which is critical for passenger comfort. In contrast, subfigure (b) of both figures shows the acceleration and speed under the traditional ACC controller (IOANNOU; CHIEN, 1993). There are more noticeable oscillations and spikes in both acceleration and speed, which can lead to a less comfortable ride. Additionally, as oscillations and speed variations increase along the platoon, it becomes evident that, in this scenario, the platoon under the ACC of Ioannou and Chien (1993) is not string-stable.

Figure 33 shows the spacing error between vehicles. Subfigure (a) illustrates the performance of the proposed ACC controller, which maintains a smaller spacing error compared to the traditional ACC shown in subfigure (b). The reduced spacing error indicates that the proposed ACC is more effective at maintaining the desired headway distance, which is critical for safety and traffic flow efficiency. The traditional ACC (IOANNOU; CHIEN, 1993), with its larger and more oscillatory spacing error, shows less reliability in maintaining the set headway, potentially leading to less safe driving conditions. Additionally, the increasing error along the platoon further indicates that the traditional ACC is not string-stable in this scenario.

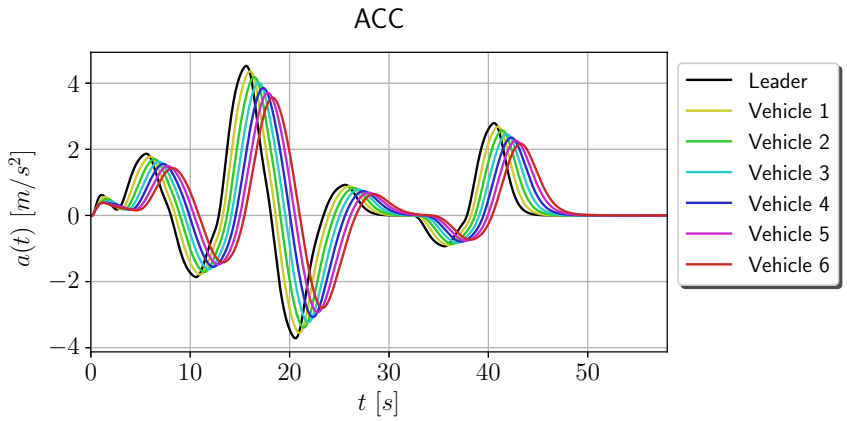

(a)

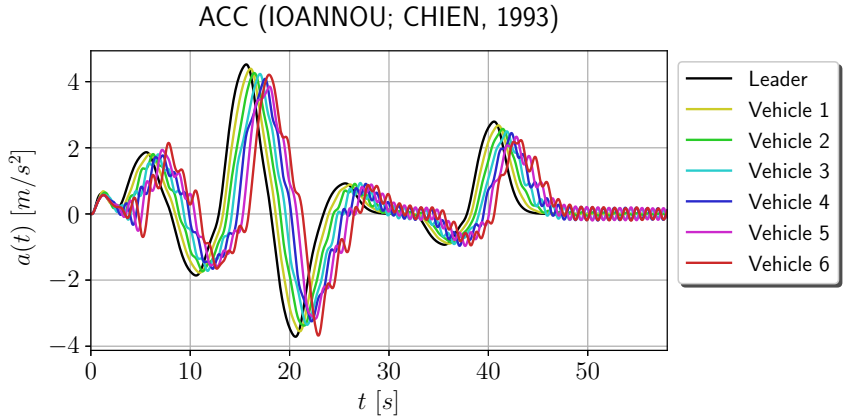

(b)

Figure 31 – The top figure (a) shows the vehicles acceleration under the proposed ACC (4.1); the bottom figure (b) shows the vehicles acceleration under ACC (IOANNOU; CHIEN, 1993) (4.2).

Figure 34 shows the jerk, which is the rate of change of acceleration. Subfigure (a) presents the jerk under the proposed ACC controller, where the values are lower. This lower jerk is advantageous as it implies smoother transitions in acceleration, enhancing passenger comfort and reducing the risk of mechanical stress on the vehicle. On the other hand, subfigure (b) displays the jerk under the traditional ACC controller (IOANNOU; CHIEN, 1993). The higher and more unpredictable jerk values suggest that the traditional ACC causes more abrupt changes in acceleration, which could lead to discomfort and increased wear on the vehicle.

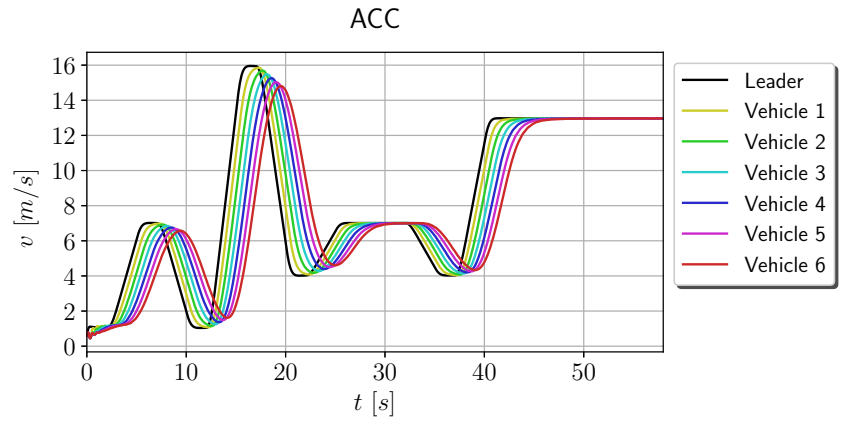

(a)

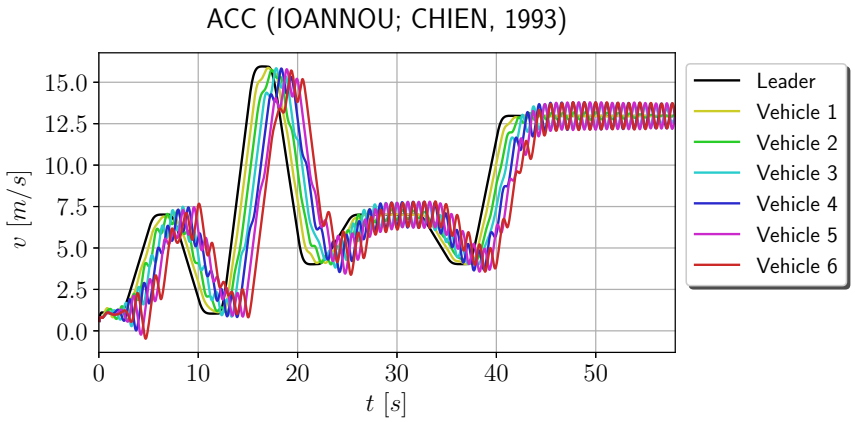

(b)

Figure 32 – The top figure (a) shows the vehicles speed under the proposed ACC (4.1); the bottom figure (b) shows the vehicles speed under ACC (IOANNOU; CHIEN, 1993) (4.2).

4.4 Bode Diagram Analysis of Proposed and Traditional ACC

The traditional adaptive cruise control (ACC) system, while effective in certain scenarios, presents several limitations that necessitate the development of an improved approach. One significant drawback of the traditional ACC is its reliance on maintaining a time-headway h greater than or equal to twice the vehicle time constant $2\zeta_i$ to ensure string stability, as demonstrated by Rajamani (2012) and originally proposed by Swaroop (1994):

$$h \geq 2\zeta_i. \tag{4.17}$$

This constraint can limit the system performance, particularly in scenarios where

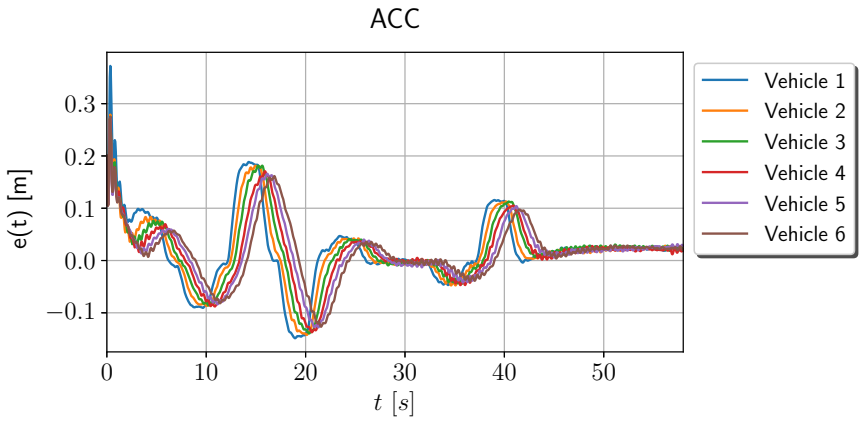

(a)

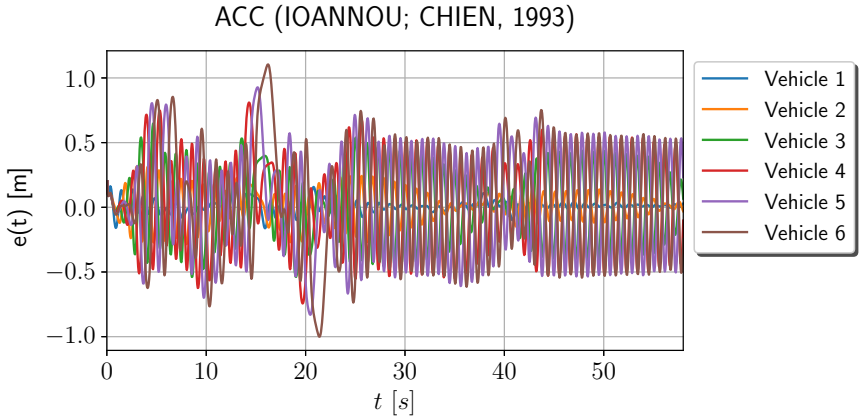

(b)

Figure 33 – The top figure (a) shows the vehicle spacing error under the proposed ACC (4.1); the bottom figure (b) shows the vehicle spacing error under ACC (IOANNOU; CHIEN, 1993) (4.2).

a smaller time-headway is desirable. In this context, to illustrate the advantages of the proposed ACC system, we present a Bode diagram analysis comparing the traditional ACC system (4.2) and the proposed ACC system (4.1).

We present the Bode diagrams for both the traditional ACC system and the proposed ACC system with a time-headway $h = 0.4$ and a vehicle time constant $\zeta_i = 0.3$. In this case, $h < 2\zeta_i$ and does not satisfy condition (4.17). The Bode diagram for the traditional ACC system, shown in Figure 35, exhibits a maximum gain greater than 1 (0 dB), indicating a potential for string instability at a particular frequency. In contrast, the Bode diagram for the proposed ACC system maintains a maximum gain within acceptable limits, ensuring string stability even with a smaller time-headway.

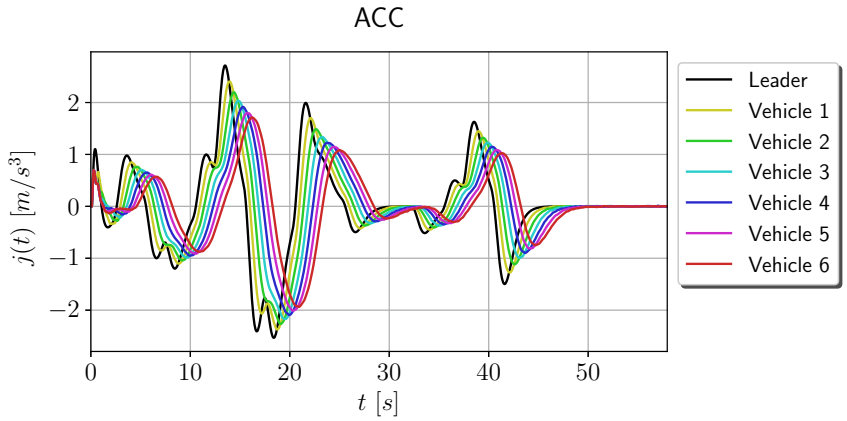

(a)

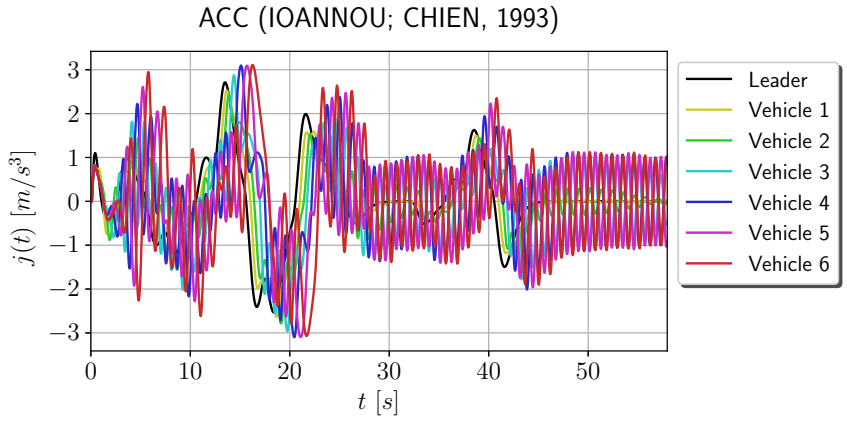

(b)

Figure 34 – The top figure (a) shows the vehicles jerk under the proposed ACC (4.1); the bottom figure (b) shows the vehicles jerk under ACC (IOANNOU; CHIEN, 1993) (4.2).

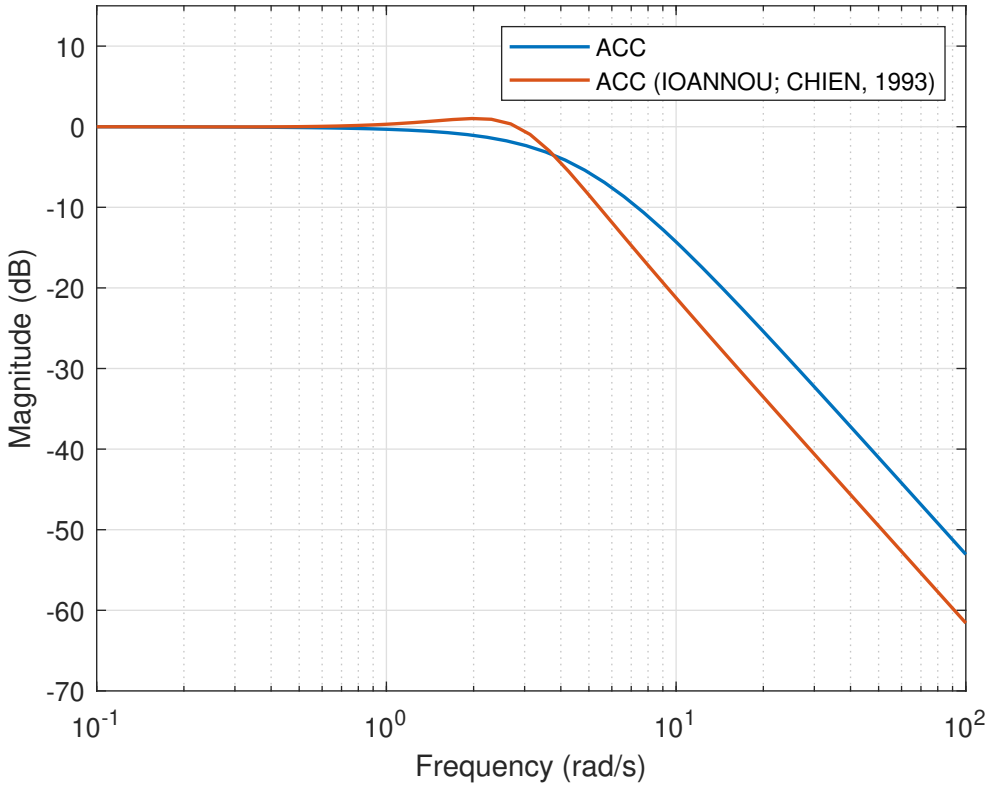

Figure 35 – Bode diagram comparing the traditional ACC (IOANNOU; CHIEN, 1993) system and the proposed ACC system with $h = 0.4$ and $\zeta_i = 0.3$.

Chapter 5

Conclusions and Future Directions

This chapter presents the conclusions of the work and suggestions for future research to be developed.

5.1 Conclusions

This thesis has explored innovative approaches to enhancing vehicle platoon systems through advanced control strategies that do not rely on wireless communication. By focusing on cooperative and adaptive cruise control (CACC and ACC) systems, the work addresses critical issues related to communication failures and latency, aiming to improve safety, efficiency, and performance in vehicle platooning. The proposed methodologies are validated through simulations in MATLAB® and Simulink®, which provide a controlled environment to verify theoretical developments, and realistic simulations using the CARLA Simulator, which accurately replicates vehicle dynamics and environmental interactions. These simulations demonstrate the practical applicability of the proposed control strategies, showcasing their potential for real-world implementation.

In Chapter 3, a new linear feedback control law that does not rely on the preceding vehicle acceleration measurement is established to ensure internal and string stability of vehicle platoon systems. To this end, we replaced the preceding vehicle acceleration signal in an efficient degraded cooperative adaptive cruise control (d-CACC) with its estimation obtained from first-order backward finite difference approximation. The main advantage of the proposed controller is that it can be computed only by onboard measurements in each vehicle, thus eliminating the need for wireless communication devices, which mitigates wireless latency issues and benefits implementation. The proposed design methodology is derived on frequency domain. First, internal and string stability conditions are developed. Then, with these results in hand, a systematic methodology to design the controller parameters is introduced as a step-by-step algorithm. These concepts are validated using

MATLAB® simulations, which show that the proposed d-CACC outperforms the CACC when subject to delays, and the CARLA Simulator with nonlinear dynamics in scenarios of fallback from CACC to d-CACC, including measurement noise, providing a high level of realism in vehicle dynamics and environmental interactions, further demonstrating the practical effectiveness of the proposed controller.

In Chapter 4, building on the ideas proposed in Chapter 3, a new ACC control law is introduced. The new formulation, like other ACC control laws, includes the speed difference between subsequent vehicles, but it also incorporates the acceleration of the own vehicle and excludes the acceleration of the preceding vehicle. Again, the control law for ACC systems does not use wireless communication between vehicles. The resulting closed-loop dynamics do not depend on the vehicle driveline dynamics; therefore, the proposed methodology, unlike traditional ACC methods, can be applied to large-scale heterogeneous vehicle platoon systems without decreasing performance. The controller gains designed via the LMI approach ensure internal and string stability. Furthermore, due to $\mathcal{D}$-region pole placement, the controller offers the possibility of setting a transient response that, in practice, does not cause discomfort to the vehicle occupants. Simulations are performed in MATLAB® and Simulink®, demonstrating that, despite using only measured states without wireless communication between vehicles, the achieved performance approximates that of CACC systems. Realistic simulations using the CARLA Simulator show that the proposed ACC outperforms traditional ACC in simulated scenarios, validating the robustness and effectiveness of the proposed control strategy under realistic driving conditions.

Despite the advancements proposed in this work, aiming to provide alternatives when wireless communication fails or is unavailable, it is acknowledged that CACC systems have the potential for the best performance among platoon control ADAS when operating with full wireless communication capabilities. This enhances roadway capacity and the efficiency of vehicles in longitudinal formations by reducing the distance between vehicles. However, there remains significant room for research and development to improve the performance of systems that do not rely on wireless communication. These systems can serve as viable alternatives while CACC technology is not yet widely adopted or when communication failures occur.

In conclusion, while the proposed control laws demonstrate significant potential and effectiveness, ongoing research is essential to further refine these systems and ensure their robustness and reliability in various scenarios. The advancements presented in this thesis contribute to the development of safer and more efficient vehicle platoon systems. Therefore, this work helps pave the way for future advancements in vehicle platoon control, aiming towards fully autonomous, and interconnected transportation systems.

5.2 Published Works

The research presented in this thesis has resulted in the following peer-reviewed publications in highly relevant journals in the field:

- M. P. S. de Abreu, F. S. S. de Oliveira, and F. O. Souza, "d-CACC for Vehicle Platoons Lacking Acceleration Signal," *IEEE Transactions on Intelligent Transportation Systems*, 2024. Publisher: IEEE (ABREU; OLIVEIRA; SOUZA, 2024b).
- M. P. S. de Abreu, F. S. S. de Oliveira, and F. O. Souza, "An improved adaptive cruise control law," *Robotics and Autonomous Systems*, vol. 176, pp. 104679, 2024. Publisher: Elsevier (ABREU; OLIVEIRA; SOUZA, 2024a).

5.3 Future Directions

Building on the research and findings presented in this thesis, several promising directions for future work are identified. An important area for future research is the development of robust control strategies that incorporate uncertainties before the linearization of the model. The current literature often addresses uncertainties in already linearized models, as seen in Chehardoli (2020), Abdullahi and Akkaya (2020), Zhu, Zhao and Zhong (2018), which may not be ideal because it simplifies the problem and can miss critical aspects of the system dynamics. Exploring effective ways to address these uncertainties in the original nonlinear models, such as uncertainties in vehicle mass, driveline dynamics, communication delays, and actuation delays, could significantly enhance the robustness and performance of vehicle platoon systems.

There is a need for updated and comprehensive reviews and surveys that compile and analyze the past and future of ACC and CACC systems. These reviews should cover various topologies, as well as different definitions and criteria for string stability and their impact on system performance. A thorough analysis of existing spacing policies and the development of new policies that evaluate safety and efficiency is also essential. Additionally, integrating systematic control methodologies within these reviews would provide a structured approach to evaluating various control strategies. Finally, an updated review that consolidates and relates these various aspects influencing the development and performance of ACC and CACC systems would be a valuable contribution and fill a gap in the current literature.

Further research could also focus on simulating the proposed controllers in varied environments, including adverse weather conditions and different road types. Integrating the ACC and CACC controllers with other Advanced Driver Assistance Systems (ADAS)

like automatic braking and lane-keeping assistance could enhance the overall safety and efficiency of vehicle platoons. Additionally, investigating cybersecurity measures to protect CACC systems from attacks that could compromise vehicle-to-vehicle communication is an important area for future work.

These future directions aim to advance the field of vehicle platoon control, contributing to the development of safer and more efficient transportation systems.

References

ABDULLAHI, A.; AKKAYA, S. Adaptive cruise control: A model reference adaptive control approach. In: IEEE. *2020 24th International Conference on System Theory, Control and Computing (ICSTCC)*. [S.l.], 2020. p. 904–908.

ABREU, M. P. de; OLIVEIRA, F. S. de; SOUZA, F. O. An improved adaptive cruise control law. *Robotics and Autonomous Systems*, Elsevier, v. 176, p. 104679, 2024.

ABREU, M. P. S. de; OLIVEIRA, F. S. S. de; SOUZA, F. de O. d-CACC for vehicle platoons lacking acceleration signal. *IEEE Transactions on Intelligent Transportation Systems*, IEEE, 2024.

AL-JHAYYISH, A. M. H.; SCHMIDT, K. W. Feedforward strategies for cooperative adaptive cruise control in heterogeneous vehicle strings. *IEEE Transactions on Intelligent Transportation Systems*, Institute of Electrical and Electronics Engineers (IEEE), v. 19, n. 1, p. 113–122, jan. 2018.

ALAM, A. A.; GATTAMI, A.; JOHANSSON, K. H. An experimental study on the fuel reduction potential of heavy duty vehicle platooning. In: IEEE. *13th international IEEE conference on intelligent transportation systems*. [S.l.], 2010. p. 306–311.

ALONSO, L. et al. Genetically tuned controller of an adaptive cruise control for urban traffic based on ultrasounds. In: SPRINGER. *Artificial Neural Networks–ICANN 2010: 20th International Conference, Thessaloniki, Greece, September 15-18, 2010, Proceedings, Part II 20*. [S.l.], 2010. p. 479–485.

AREM, B. V.; DRIEL, C. J. V.; VISSER, R. The impact of cooperative adaptive cruise control on traffic-flow characteristics. *IEEE Transactions on intelligent transportation systems*, IEEE, v. 7, n. 4, p. 429–436, 2006.

BERTOZZI, M.; BROGGI, A.; FASCIOLI, A. Vision-based intelligent vehicles: State of the art and perspectives. *Robotics and Autonomous systems*, Elsevier, v. 32, n. 1, p. 1–16, 2000.

BOYD, S. et al. *Linear Matrix Inequalities in System and Control Theory*. [S.l.]: Society for Industrial and Applied Mathematics, 1994.

CAO, Z. et al. End-to-end adaptive cruise control based on timing network. In: SPRINGER. *Proceedings of the 19th Asia Pacific Automotive Engineering Conference & SAE-China Congress 2017: Selected Papers*. [S.l.], 2019. p. 839–852.

CAUDILL, R. J.; GARRARD, W. L. Vehicle-follower longitudinal control for automated transit vehicles. *Journal of Dynamic Systems, Measurement, and Control*, ASME International, v. 99, n. 4, p. 241–248, dez. 1977.

CHEHARDOLI, H. Robust optimal control and identification of adaptive cruise control systems in the presence of time delay and parameter uncertainties. *Journal of Vibration and Control*, SAGE Publications Sage UK: London, England, v. 26, n. 17-18, p. 1590–1601, 2020.

CHEN, X.-w. et al. Research on the intelligent control and simulation of automobile cruise system based on fuzzy system. *Mathematical problems in engineering*, Hindawi, v. 2016, 2016.

CHENG, J.; JIA, X. Z.; WANG, Y. B. Numerical differentiation and its applications. *Inverse Problems in Science and Engineering*, v. 15, n. 4, p. 339–357, 2007.

Chilali, M.; Gahinet, P. H_∞ design with pole placement constraints: an LMI approach. *IEEE Transactions on Automatic Control*, v. 41, n. 3, p. 358–367, 1996.

DARBHA, S.; KONDURI, S.; PAGILLA, P. R. Benefits of v2v communication for autonomous and connected vehicles. *IEEE Transactions on Intelligent Transportation Systems*, IEEE, v. 20, n. 5, p. 1954–1963, 2018.

DARBHA, S.; RAJAGOPAL, K.; TYAGI, V. A review of mathematical models for the flow of traffic and some recent results. *Nonlinear analysis: Theory, methods & applications*, Elsevier, v. 69, n. 3, p. 950–970, 2008.

DAVILA, A.; ARAMBURU, E.; FREIXAS, A. Making the best out of aerodynamics: Platoons. In: . [S.l.: s.n.], 2013.

DEY, K. C. et al. Vehicle-to-vehicle (v2v) and vehicle-to-infrastructure (v2i) communication in a heterogeneous wireless network–performance evaluation. *Transportation Research Part C: Emerging Technologies*, Elsevier, v. 68, p. 168–184, 2016.

DOSOVITSKIY Alexey et al. CARLA: An open urban driving simulator. In: *Proc. of the 1st Annual Conf. on Robot Learning*. [S.l.: s.n.], 2017. p. 1–16.

EMIRLER, M. T.; GÜVENÇ, L.; GÜVENÇ, B. A. Design and evaluation of robust cooperative adaptive cruise control systems in parameter space. *International Journal of Automotive Technology*, Springer, v. 19, n. 2, p. 359–367, 2018.

ESKANDARIAN, A.; WU, C.; SUN, C. Research advances and challenges of autonomous and connected ground vehicles. *IEEE Transactions on Intelligent Transportation Systems*, Institute of Electrical and Electronics Engineers (IEEE), v. 22, n. 2, p. 683–711, fev. 2021.

FANCHER, P. Research on desirable adaptive cruise control behavior in traffic streams. In: . [S.l.: s.n.], 2003.

FENG, S. et al. String stability for vehicular platoon control: Definitions and analysis methods. *Annual Reviews in Control*, Elsevier BV, v. 47, p. 81–97, 2019.

GAO, F. et al. A decoupling method for distributed control of vehicular platoons with V2V. In: *IET International Conference on Intelligent and Connected Vehicles (ICV 2016)*. [S.l.: s.n.], 2016. p. 1–6.

GARRARD, W. et al. State-of-the-art of longitudinal control of automated guideway transit vehicles. *High Speed Ground Transp J*, John Wiley and Sons Ltd, v. 12, n. 2, p. 35–67, 1978.

GHASEMI, A.; KAZEMI, R.; AZADI, S. Stable decentralized control of a platoon of vehicles with heterogeneous information feedback. *IEEE Transactions on Vehicular Technology*, IEEE, v. 62, n. 9, p. 4299–4308, 2013.

GODINHO, D. A. et al. Control and reorganization of heterogeneous vehicle platoons after vehicle exits and entrances. *International Journal of Control, Automation and Systems*, Springer, v. 20, n. 8, p. 2437–2446, 2022.

GODINHO, D. A. et al. A strategy for traffic safety of vehicular platoons under connection loss and time-delay. *IEEE Transactions on Intelligent Transportation Systems*, IEEE, v. 24, n. 6, p. 6627–6638, 2023.

GONG, S.; ZHOU, A.; PEETA, S. Cooperative adaptive cruise control for a platoon of connected and autonomous vehicles considering dynamic information flow topology. *Transportation research record*, SAGE Publications Sage CA: Los Angeles, CA, v. 2673, n. 10, p. 185–198, 2019.

GÜLDEN, B.; EMIRLER, M. T. Investigation of different communication topologies for cooperative adaptive cruise control systems. *International Journal of Automotive Science And Technology*, Otomotiv Mühendisleri Derneği, v. 8, n. 1, p. 150–158, 2024.

GUNTER, G. et al. Are commercially implemented adaptive cruise control systems string stable? *IEEE Transactions on Intelligent Transportation Systems*, IEEE, 2020.

HANKE, M.; SCHERZER, O. Inverse problems light: Numerical differentiation. *The American Mathematical Monthly*, v. 108, n. 6, p. 512–521, 2001.

HAYATI, H. et al. Jerk within the context of science and engineering—a systematic review. *Vibration*, MDPI, v. 3, n. 4, p. 371–409, 2020.

HIDAYATULLAH, M. R.; JUANG, J.-C. Adaptive cruise control with gain scheduling technique under varying vehicle mass. *IEEE Access*, IEEE, v. 9, p. 144241–144256, 2021.

IOANNOU, P. A.; CHIEN, C.-C. Autonomous intelligent cruise control. *IEEE Transactions on Vehicular technology*, IEEE, v. 42, n. 4, p. 657–672, 1993.

JIA, D. et al. A survey on platoon-based vehicular cyber-physical systems. *IEEE Communications Surveys & Tutorials*, IEEE, v. 18, n. 1, p. 263–284, 2015.

JIANG, Y. et al. Hierarchical framework for adaptive cruise control with model predictive control method. In: . [S.l.: s.n.], 2017.

JIN, I. G.; OROSZ, G. Optimal control of connected vehicle systems with communication delay and driver reaction time. *IEEE Transactions on Intelligent Transportation Systems*, IEEE, v. 18, n. 8, p. 2056–2070, 2016.

KAYACAN, E. Multiobjective H_∞ control for string stability of cooperative adaptive cruise control systems. *IEEE Transactions on Intelligent Vehicles*, Institute of Electrical and Electronics Engineers (IEEE), v. 2, n. 1, p. 52–61, mar. 2017.

KAYACAN, E. Multiobjective H_∞ control for string stability of cooperative adaptive cruise control systems. *IEEE Transactions on Intelligent Vehicles*, IEEE, v. 2, n. 1, p. 52–61, 2017.

KHATIR, M. E.; DAVISON, E. J. Decentralized control of a large platoon of vehicles using non-identical controllers. In: IEEE. *Proceedings of the 2004 American Control Conference.* [S.l.], 2004. v. 3, p. 2769–2776.

KLANČAR, G.; MATKO, D.; BLAŽIČ, S. A control strategy for platoons of differential drive wheeled mobile robot. *Robotics and Autonomous Systems*, Elsevier, v. 59, n. 2, p. 57–64, 2011.

LEFEBER, E.; PLOEG, J.; NIJMEIJER, H. Cooperative adaptive cruise control of heterogeneous vehicle platoons. *IFAC-PapersOnLine*, Elsevier BV, v. 53, n. 2, p. 15217–15222, 2020.

LIU, Y. et al. Internal stability and string stability of connected vehicle systems with time delays. *IEEE Transactions on Intelligent Transportation Systems*, Institute of Electrical and Electronics Engineers (IEEE), p. 1–13, 2020.

LOUISELL, J. A matrix method for determining the imaginary axis eigenvalues of a delay system. *IEEE Transactions on Automatic Control*, v. 46, n. 12, p. 2008–2012, 2001.

MAO, J. et al. Research on vehicle adaptive cruise control method based on fuzzy model predictive control. *Machines*, MDPI, v. 9, n. 8, p. 160, 2021.

MOSHARAFIAN, S. et al. Gaussian process based stochastic model predictive control for cooperative adaptive cruise control. In: IEEE. *2021 IEEE Vehicular Networking Conference (VNC).* [S.l.], 2021. p. 17–23.

NAUS, G. J. L. et al. String-stable CACC design and experimental validation: A frequency-domain approach. *IEEE Transactions on Vehicular Technology*, Institute of Electrical and Electronics Engineers (IEEE), v. 59, n. 9, p. 4268–4279, nov. 2010.

NETO, A. A.; MOZELLI, L. A. Robust longitudinal control for vehicular platoons using deep reinforcement learning. *IEEE Transactions on Intelligent Transportation Systems*, IEEE, 2024.

NETO, A. A.; MOZELLI, L. A.; SOUZA, F. O. Control of air-ground convoy subject to communication time delay. *Computers & Electrical Engineering*, Elsevier, v. 76, p. 213–224, 2019.

NOOR-A-RAHIM, M. et al. 6g for vehicle-to-everything (v2x) communications: Enabling technologies, challenges, and opportunities. *Proceedings of the IEEE*, IEEE, v. 110, n. 6, p. 712–734, 2022.

PATOUNAS, G.; ZHANG, Y.; GJESSING, S. Evaluating defence schemes against jamming in vehicle platoon networks. In: *2015 IEEE 18th International Conference on Intelligent Transportation Systems.* [S.l.: s.n.], 2015. p. 2153–2158.

PEPPARD, L. String stability of relative-motion PID vehicle control systems. *IEEE Transactions on Automatic Control*, IEEE, v. 19, n. 5, p. 579–581, 1974.

PLOEG, J. et al. Graceful degradation of cooperative adaptive cruise control. *IEEE Transactions on Intelligent Transportation Systems*, Institute of Electrical and Electronics Engineers (IEEE), v. 16, n. 1, p. 488–497, fev. 2015.

PLOEG, J. et al. Controller synthesis for string stability of vehicle platoons. *IEEE Transactions on Intelligent Transportation Systems*, Institute of Electrical and Electronics Engineers (IEEE), v. 15, n. 2, p. 854–865, abr. 2014.

PLOEG, J.; WOUW, N. van de; NIJMEIJER, H. L_p string stability of cascaded systems: Application to vehicle platooning. *IEEE Transactions on Control Systems Technology*, Institute of Electrical and Electronics Engineers (IEEE), v. 22, n. 2, p. 786–793, mar. 2014.

RAJAMANI, R. *Vehicle Dynamics and Control*. [S.l.]: Springer US, 2012.

RAMYAR, S.; HOMAIFAR, A. Impact of unreliable communication on string stability of cooperative adaptive cruise control. In: IEEE. *2019 IEEE International Conference on Systems, Man and Cybernetics (SMC)*. [S.l.], 2019. p. 4263–4268.

ROGGE, J. A.; AEYELS, D. Vehicle platoons through ring coupling. *IEEE Transactions on Automatic Control*, IEEE, v. 53, n. 6, p. 1370–1377, 2008.

ROSA, F. D. et al. Sliding mode acceleration estimation for safe vehicular cooperative adaptive cruise control. In: IEEE. *2022 IEEE 25th International Conference on Intelligent Transportation Systems (ITSC)*. [S.l.], 2022. p. 2028–2033.

SAWANT, J.; CHASKAR, U.; GINOYA, D. Robust control of cooperative adaptive cruise control in the absence of information about preceding vehicle acceleration. *IEEE Transactions on Intelligent Transportation Systems*, Institute of Electrical and Electronics Engineers (IEEE), v. 22, n. 9, p. 5589–5598, set. 2021.

SCHMIED, R.; COLANERI, P. Mixed H_2-H_∞ control for automated highway driving. *Mechatronics*, Elsevier, v. 57, p. 63–72, 2019.

SEILER, P.; PANT, A.; HEDRICK, K. Disturbance propagation in vehicle strings. *IEEE Transactions on Automatic Control*, Institute of Electrical and Electronics Engineers (IEEE), v. 49, n. 10, p. 1835–1841, out. 2004.

SHAKOURI, P.; ORDYS, A. Nonlinear model predictive control approach in design of adaptive cruise control with automated switching to cruise control. *Control Engineering Practice*, Elsevier, v. 26, p. 160–177, 2014.

SIEBERT, F. W.; OEHL, M.; PFISTER, H.-R. The influence of time headway on subjective driver states in adaptive cruise control. *Transportation research part F: traffic psychology and behaviour*, Elsevier, v. 25, p. 65–73, 2014.

SOUZA, F. de O. Imaginary characteristic roots of neutral systems with commensurate delays. *Systems & Control Letters*, Elsevier, v. 127, p. 19–24, 2019.

SOUZA, F. O. et al. Stability and formation error of homogeneous vehicular platoons with communication time delays. *IEEE Transactions on Intelligent Transportation Systems*, p. 1–12, 2019.

STANKOVIC, S. S.; STANOJEVIC, M. J.; SILJAK, D. D. Decentralized overlapping control of a platoon of vehicles. *IEEE Transactions on Control Systems Technology*, IEEE, v. 8, n. 5, p. 816–832, 2000.

STüDLI, S.; SERON, M.; MIDDLETON, R. From vehicular platoons to general networked systems: String stability and related concepts. *Annual Reviews in Control*, Elsevier BV, v. 44, p. 157–172, 2017.

SWAROOP, D. *String stability of interconnected systems: An application to platooning in automated highway systems*. [S.l.]: University of California, Berkeley, 1994.

SWAROOP, D.; HEDRICK, J. String stability of interconnected systems. *IEEE Transactions on Automatic Control*, Institute of Electrical and Electronics Engineers (IEEE), v. 41, n. 3, p. 349–357, mar. 1996.

SWAROOP, D. et al. A comparision of spacing and headway control laws for automatically controlled vehicles1. *Vehicle system dynamics*, Taylor & Francis, v. 23, n. 1, p. 597–625, 1994.

TIAN, B. et al. Communication delay compensation for string stability of CACC system using LSTM prediction. *Vehicular Communications*, Elsevier, v. 29, p. 100333, 2021.

TIGANASU, A. et al. Comparative analysis of advanced cooperative adaptive cruise control algorithms for vehicular cyber physical systems. *Journal of Control Engineering and Applied Informatics*, v. 23, n. 1, p. 82–92, 2021.

TORRENT-MORENO, M. et al. Vehicle-to-vehicle communication: Fair transmit power control for safety-critical information. *IEEE Transactions on Vehicular Technology*, v. 58, n. 7, p. 3684–3703, 2009.

WANG, J. et al. A survey of vehicle to everything (v2x) testing. *Sensors*, MDPI, v. 19, n. 2, p. 334, 2019.

WANG, Z. et al. A survey on cooperative longitudinal motion control of multiple connected and automated vehicles. *IEEE Intelligent Transportation Systems Magazine*, Institute of Electrical and Electronics Engineers (IEEE), v. 12, n. 1, p. 4–24, 2020.

WANG, Z.; WU, G.; BARTH, M. J. A review on cooperative adaptive cruise control (CACC) systems: Architectures, controls, and applications. In: IEEE. *2018 21st International Conference on Intelligent Transportation Systems (ITSC)*. [S.l.], 2018. p. 2884–2891.

WIT, C. C. D.; BROGLIATO, B. Stability issues for vehicle platooning in automated highway systems. In: IEEE. *Proceedings of the 1999 IEEE International Conference on Control Applications (Cat. No. 99CH36328)*. [S.l.], 1999. v. 2, p. 1377–1382.

WU, C.; LIN, Y.; ESKANDARIAN, A. Cooperative adaptive cruise control with adaptive Kalman filter subject to temporary communication loss. *IEEE Access*, IEEE, v. 7, p. 93558–93568, 2019.

WU, C. et al. Spacing policies for adaptive cruise control: A survey. *IEEE Access*, IEEE, v. 8, p. 50149–50162, 2020.

YU, L.; WANG, R. Researches on adaptive cruise control system: A state of the art review. *Proceedings of the Institution of Mechanical Engineers, Part D: Journal of Automobile Engineering*, SAGE Publications Sage UK: London, England, v. 236, n. 2-3, p. 211–240, 2022.

ZHAO, C. et al. Vehicle platooning with non-ideal communication networks. *IEEE transactions on vehicular technology*, IEEE, v. 70, n. 1, p. 18–32, 2020.

ZHENG, Y. et al. Stability and scalability of homogeneous vehicular platoon: Study on the influence of information flow topologies. *IEEE Transactions on intelligent transportation systems*, IEEE, v. 17, n. 1, p. 14–26, 2015.

ZHU, Y.; HE, H.; ZHAO, D. LMI-based synthesis of string-stable controller for cooperative adaptive cruise control. *IEEE Transactions on Intelligent Transportation Systems*, IEEE, v. 21, n. 11, p. 4516–4525, 2019.

ZHU, Y.; ZHAO, D.; HE, H. Synthesis of cooperative adaptive cruise control with feedforward strategies. *IEEE Transactions on Vehicular Technology*, Institute of Electrical and Electronics Engineers (IEEE), v. 69, n. 4, p. 3615–3627, abr. 2020.

ZHU, Y.; ZHAO, D.; ZHONG, Z. Adaptive optimal control of heterogeneous CACC system with uncertain dynamics. *IEEE Transactions on Control Systems Technology*, IEEE, v. 27, n. 4, p. 1772–1779, 2018.